A Benzothiadiazole-based Covalent Organic Framework for Highly Efficient Visible Light-Mediated Heterogeneous Photocatalysis

Sakil Mallick

A dissertation submitted for the partial fulfillment of an MS degree in Science

Indian Institute of Science Education and Research Mohali

April 2022

Certificate of Examination

This is to certify that the dissertation titled "**A Benzothiadiazole-based Covalent Organic Framework for Highly Efficient Visible Light-Mediated Heterogeneous Photocatalysis**" submitted by **Sakil Mallick** (MP19007) for the partial fulfillment of the MS degree program of the Institute, has been examined by the thesis committee duly appointed by the Institute. The committee finds the work done by the candidate satisfactory and recommends that the report be accepted.

Dr. Raj Kumar Roy Dr. Subhabrata Maiti Dr. Santanu Kumar Pal

(Supervisor)

Dated: April 28, 2022

Declaration

The work presented in this dissertation has been carried out by me under the guidance of Dr. Santanu Kumar Pal at the Indian Institute of Science Education and Research Mohali.

This work has not been submitted in part or in full for a degree, a diploma, or a fellowship to any other university or institute. Whenever contributions of others are involved, every effort is made to indicate this clearly, with due acknowledgment of collaborative research and discussions. This thesis is a bonafide record of original work done by me and all sources listed within have been detailed in the bibliography.

Sakil Mallick

(MP19007)

Dated: April 28, 2022

In my capacity as the supervisor of the candidate's project work, I certify that the above statements by the candidate are true to the best of my knowledge.

Dr. Santanu Kumar Pal

(Supervisor)

Acknowledgment

First and foremost, I praise and thank the almighty for being the unfailing source of support, comfort, and strength throughout the completion of my project work.

I would like to thank Prof. Jayaraman Gowrishankar, Director, Indian Institute of Science Education and Research Mohali, and Dr. Sanjay Singh, Head of Department of Chemical Science, for the infrastructure, library facilities, research facilities, NMR facilities, and for exposing me to the working environment of a full-fledged research institute.

It’s an honor and proud privilege in expressing my deepest gratitude to Dr. Santanu Kumar Pal, Associate Professor, Department of Chemical Science, Indian Institute of Science Education and Research Mohali, for his kindness and support, for accepting my request to work under his guidance, for enabling me in the pursuit of my career.

I express my warm appreciation and most respectful regards to Dr. Raj Kumar Roy and Dr. Subhabrata Maiti, my thesis committee members for their valuable suggestions and comments during the committee meetings.

I am so obliged and extremely thankful to Mr. Yogendra Nailwal for patiently teaching me everything from the basics. He directed me through this assignment by offering me significant intellectual input when I needed it the most, assisting me when I got off track, and clarifying me when I was perplexed. This idea would simply be a dream without his assistance and efforts.

In addition, I'd like to thank my former and present lab mates for their insightful conversations and cooperation.

Mr. Balbir and Mr. Triveni, as well as the chemistry teaching lab assistants, are also to be thanked for their assistance during my study time.

All of my dear friends, particularly Nirmal Malik, Alokananda Chanda, Monojit Roy, Shikha, Arjun, and Sourav deserve my gratitude. They supported me through all of my difficulties and expressed my sorrows and joys on several occasions.

Last but most significantly, it gives me great joy to express my gratitude to my family members, who have always believed in me and helped me unconditionally throughout my life.

Sakil Mallick

List of Figures

List of Tables

List of Schemes

Abbreviations

COF	Covalent Organic Framework
MOF	Metal-Organic Framework
CMP	Conjugated Microporous Polymer
BTD-CHO	Di-(benzothiadiazole-4,7-diyl)di-benzaldehyde
TAPT	1,3,5-tris-(4-aminophenyl)triazine
TAA	1,3,5,7-tetraaminoadamantane
TAPM	Tetra-(4-aminophenyl)methane
o-DCB	*o*-dichloro benzene
DMAc	Dimethylacetamide
THF	Tetrahydrofuran
FT-IR	Fourier Transform Infrared Spectroscopy
PXRD	Powder X-ray Diffraction
SEM	Scanning Electron Microscope
TEM	Transmission Electron Microscope
TGA	Thermogravimetric Analysis

Contents

Abstract

In recent years, the synthesis and design of porous organic materials have gained huge interest because of their extraordinary properties such as very high BET surface area, high chemical and thermal stability, low density, and inherent properties of building units. These porous organic materials are constructed by purely organic building units connected via strong covalent bonds to form an ordered framework. Covalent organic frameworks (COFs) are a kind of porous organic material that exhibits crystallinity and porosity. These fully conjugated materials show exceptional applications in biological medicine, sensing, gas adsorption and separation, optoelectronics, and catalysis. In general, COFs' diverse uses are due to their versatile molecular design and synthetic techniques, broad conjugated degrees, band structure, heteroatoms, and porous features.

The motive of the study is to synthesize a benzothiadiazole-based COF to reduce the band gap between the valence band (VB) and conduction band (CB) of the resultant framework. A crystalline benzothiadiazole-based (TAPT-BTD-COF) was synthesized by the Schiff-based condensation reaction between the monomers TAPT and BTD-CHO. Furthermore, TAPT-BTD-COF was used as a heterogeneous catalyst for the oxidative coupling reaction between *o*-phenylenediamine and aromatic aldehydes under visible-light conditions with excellent yield.

The first chapter of the thesis deals with a brief introduction, design, and applications of COFs. The second chapter contains the synthetic schemes, experimental procedures, and basic characterizations of TAPT-BTD-COF.

Chapter 1

1.1 Introduction

In 1920, German organic chemist Hermann Staudinger illustrated the existence of higher molecular weight, which was termed *macromolecules*. Later, this was known as a polymer. The first 100 years of synthetic polymerization does dominate by two structural paradigms: topologically linear chains and amorphous polymer.[1-2] Initially, it was believed that these interactions between amphiphilic substances would result in two-dimensional polymers, but they most likely resulted in irregularly cross-linked polymers. Despite this early enthusiasm for two-dimensional (2D) polymerization, the synthetic and analytical capabilities available at the time were insufficient to achieve this aim without difficulty. Polymer chemists, often known as chain builders, are a subculture of organic chemists who have mastered one-dimensional control, but in 2D and 3D, it is a synthetic wasteland. The polymer structure mainly depends on the control of the chain conformation using a covalent bond. 2D porous polymers are known as "2D" due to their structural framework where covalent interconnection stays in-plane and non-covalent bindings between different planes are in and out-of-plane directions. It can show other orders of stacking such as antiparallel, staggered, or eclipsed due to different non-bonding interactions. These different orders of stacking would exert a particular influence on the properties and functions. In the past, the synthesis of completely inorganic material and organic-inorganic hybrid polymeric material such as perovskites, zeolites, and metal-organic frameworks (MOFs) has shown substantial progress. In 2005, Omar Yaghi discovered the first covalent organic frameworks (COFs), which were 2D crystalline porous organic polymers.[3-6] These crystalline materials follow reversible reaction kinetics by thermodynamically controlled dynamic covalent chemistry. Due to this kinetics, repair of the structural deficiencies and the creation of new bonds happen automatically. Correct structural flaws and rearrangement of the framework to provide a long-range order and crystallinity cannot be found in typical organic polymers produced by kinetically driven, irreversible bond formation processes compared to C=N-like coupling.[7] After crystalline COFs were discovered, other porous organic materials came into the picture. Conjugated microporous polymers (CMPs) are the members of porous organic polymers that have drawn considerable scientific attention owing to their vast range of applications as new functional materials. These are definite classes of materials that can assemble by π-π interactions and can form extended structures with microporous skeleton and amorphous

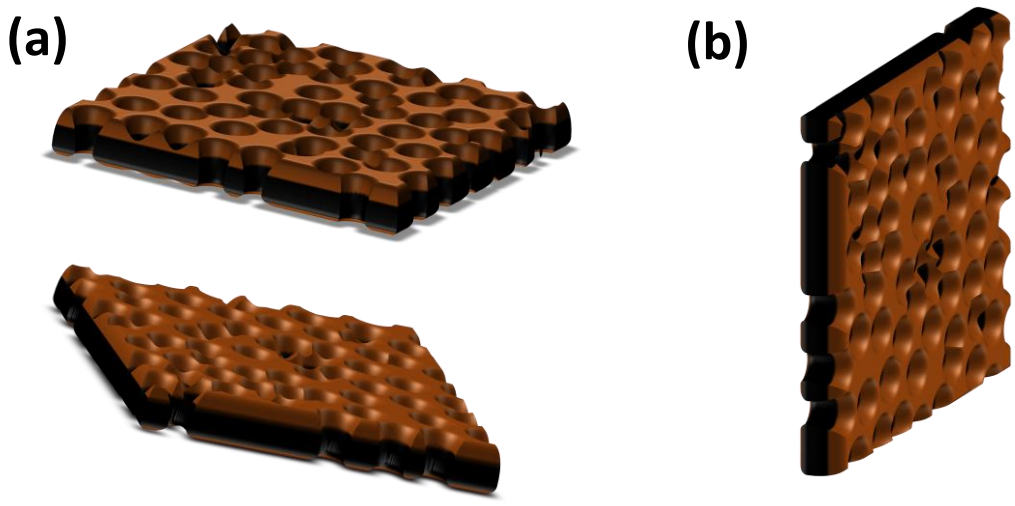

Figure 1. The appearance of porous materials (a) horizontally, (b) vertically. Redrawn from reference[8]

crystallinity.[9-10] Figure 1 shows the appearance of the porous materials.

Covalent organic frameworks (COFs) are crystalline porous polymeric materials with a layered structure, unique pore size order, programmable topologies, and excellent chemically and thermally stable materials. It's made entirely of lightweight components and could be more durable. For this reason, these materials offer diverse potential applications in different fields.[11-12] These materials could be used as a host-guest interaction because of the porosity present in their structure. The donor-acceptor interaction could also be introduced in the COFs skeleton for various purposes. The fully conjugated porous polymeric structure is constructed by dynamic covalent chemistry (DCC) principles in COFs. Strong covalent bonds directly connect the building blocks in COFs. The “crystallization problem” is the main challenge in assembling building blocks. The presence of strong covalent bonds generally leads to an amorphous material. To overcome this situation, the most important criteria is to provide the reversible condition in bond formation to prevent the creation of disordered and amorphous products. Therefore, during the crystallization process, the reversibility of bond formation provides self-healing and error correction in the resultant skeleton. Mostly, this is attained by either using solvent combinations so that the byproducts have limited solubility or through control of the pressure in the reaction vessel. The topology diagram generally directs the growth of polymeric networks, where the monomers with similar geometry are connected to construct different 2D or 3D structures with different pores. Because of these features, COFs have gained attention as a potential family of materials for applications in various areas such as heterogeneous catalysis, gas storage, and separation, sensing, ion conduction, proton

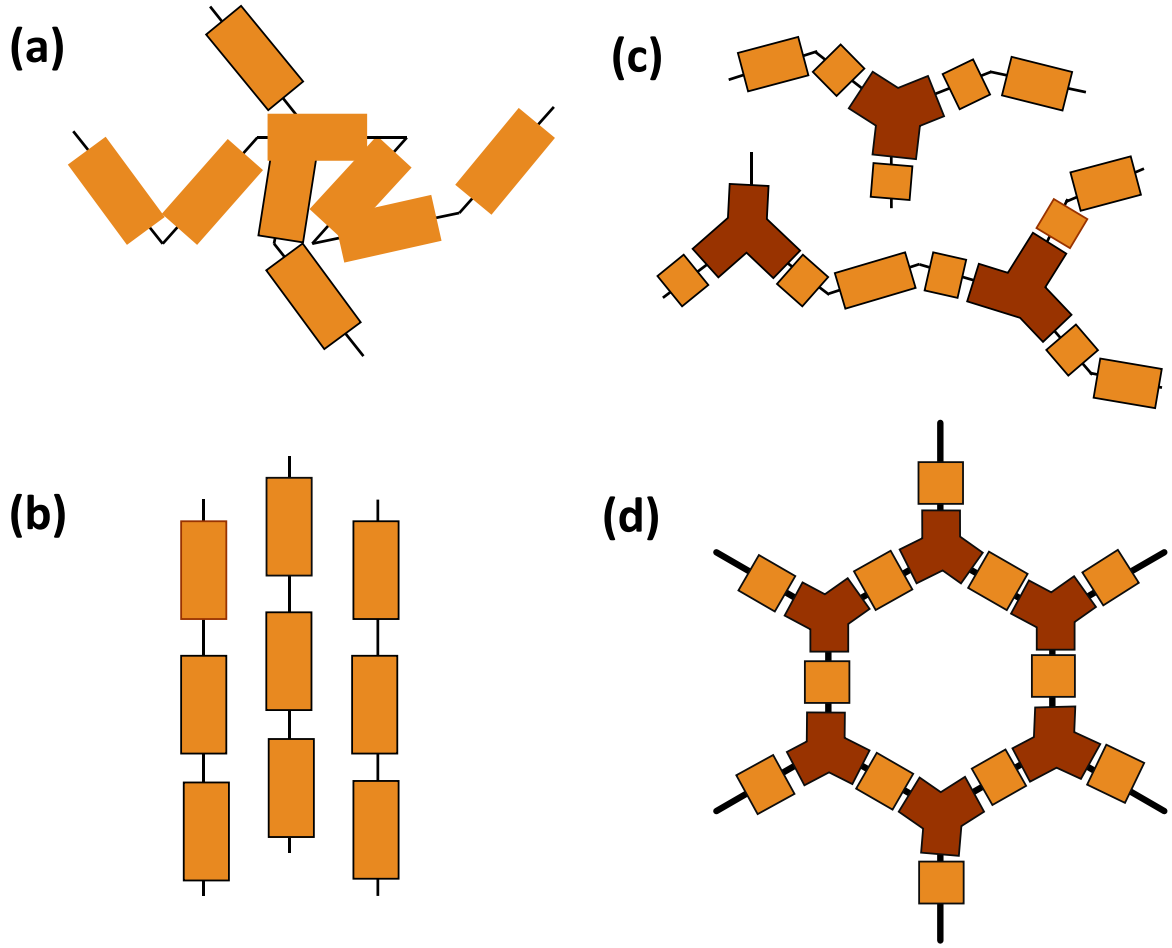

Figure 2. (a) Amorphous linear polymer, (b) Amorphous 2D polymer, (c) Crystalline linear polymer (d) Crystalline 2D polymer. Redrawn from reference[13]

conduction, optoelectronics, and so on.[14-17] Figure 2 shows the amorphous and crystalline states of materials.

1.2 Classification

Porous materials can be divided into many categories based on their constituent components. According to pore size, porous materials are branched into three categories; microporous (pore size < 2 nm), mesoporous (pore size between 2 nm – 50 nm), and macroporous (pore size > 50 nm). Based on building blocks, these materials can be classified into three categories; purely organic, inorganic-organic hybrid, and purely inorganic, as shown in Figure 3. Furthermore, purely organic frameworks can be categorized into two components based on crystallinity; crystalline organic frameworks, and amorphous organic frameworks. Polymeric intrinsic microporous (PIM), conjugated microporous polymers (CMPs), hyper-cross-linked polymers (HCPs), extrinsic porous molecules (EPMs), porous

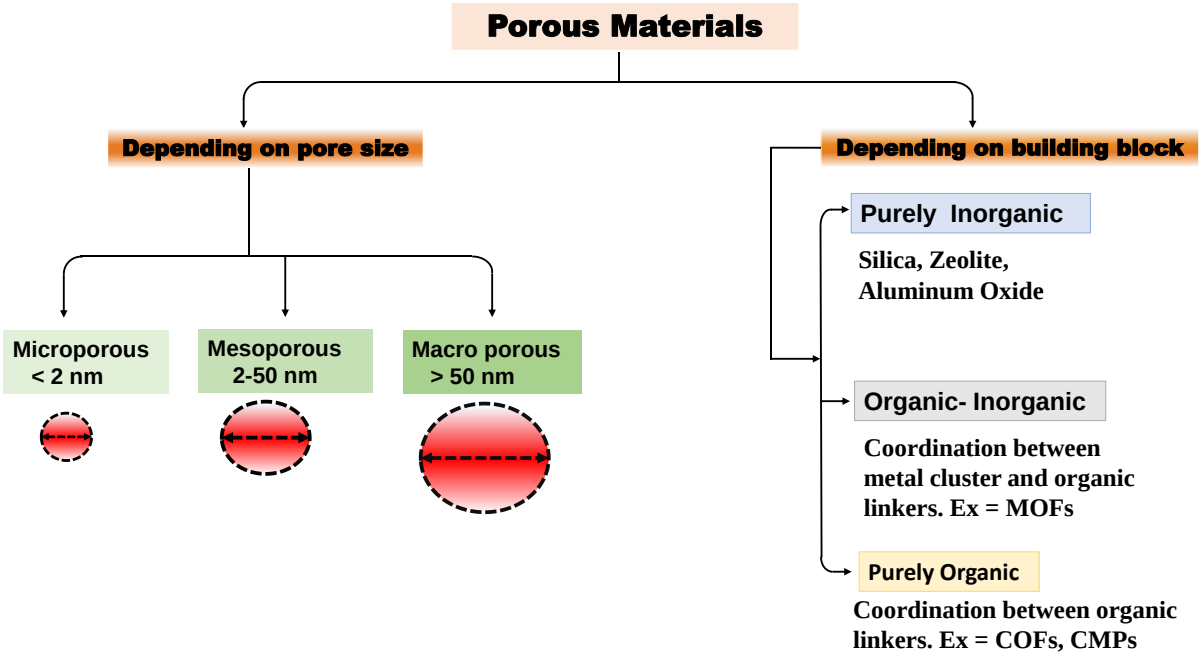

Figure 3. Classification of porous materials. Redrawn from reference[18]

aromatic frameworks (PAFs), and porous organic cages (POCs) are examples of amorphous porous materials. Covalent triazine frameworks (CTFs) and COFs are the members of ordered, crystalline materials.[19]

1.3 Design Principle

The pathway of covalent bond forming and leading to the polymer backbone development is solely dependent on the character of the topology design diagram.[20] The monomers must have rigid structures in which specific sites are arranged in a unique framework in a definite order of each covalent bond. The area between the reactive positions of each monomer is represented with the help of precise geometry.[7] The covalent bonding between monomers guides the formation of structural coordination and determines the respective positions of the succeeding rigid or flexible polymer. This diagram of topology and the monomers geometry makes the substructure improve the fundamentally ordered network. These porous organic polymers developed different shaped-based primary-order structures and various essential nanopores of distinct sizes.[9] As shown in Figure 4, planar rigid monomers outline the development of polymer networks in a two-dimensional way resulting from the formation of two-dimensional atomic layers with particular topologies. This is a pathway in which each monomer entity assembles on each other into layered structures of 2D covalent organic polymers. By stacking the 2D polymers onto one another,

the 2D COFs build high-order z-arrays. Therefore, a particular property of 2D COFs creates not only wholly ordered design but also pore channels in 1D.[21]

1.3.1 Design of 2D COFs

COFs can create complex patterns by combining or manipulating a wide range of sequences (isotropic topologies) and disarray (anisotropic topologies) of polygonal skeletons. In all cases, the lattice structure and each pore are extremely ordered, and the pores are all different. 2D COFs topologies are mainly symmetric topologies and asymmetric topologies. COFs with various skeletons and pores are generated in symmetric topologies by mixing variant monomer geometries. For instance, the association of three C_2 forms hexagonal COFs, and the combination of C_2 with C_3, C_3 with C_3, and C_6 with C_2, also generates hexagonal COFs. The topology of monomers can determine the pore size of each COFs. The linker and knot organization define the final framework; the substantiality of the toughness of interlayer bindings and the knot unit dominates the variant of topology.[3] The fragile interlayer π- π bindings between knot and linker can be originated from their twisted structures.

1.3.2 Design of 3D COFs

Covalently linked polymer backbones must have a tetrahedral or orthogonal geometry at least one building block to create 3D networks. The combination of C_3, C_2, C_4, and tetrahedral geometry achieves the different types of 3D COFs, categorized into various kinds of networks like rra, dia, pts, bor, srs, and ctn. Several-fold interpenetration is present in the 3D COFs. For this reason, 3D COFs possess lower porosity than expected.[9]

1.4 Linkages of COFs

The essence of planar building blocks of COFs essentially generate various reactive sites and maintain rigid π-backbones. The synthesis of COFs can be done by taking two different polarity solvents with different proportions. Generally, COFs have been synthesized with linkages such as triazine, hydrazone, boroxine, borosilicate, imine, borazine, boronate-ester, azine, C=C bond, amide, viologen, and urea, as shown in Figure 5.[22]

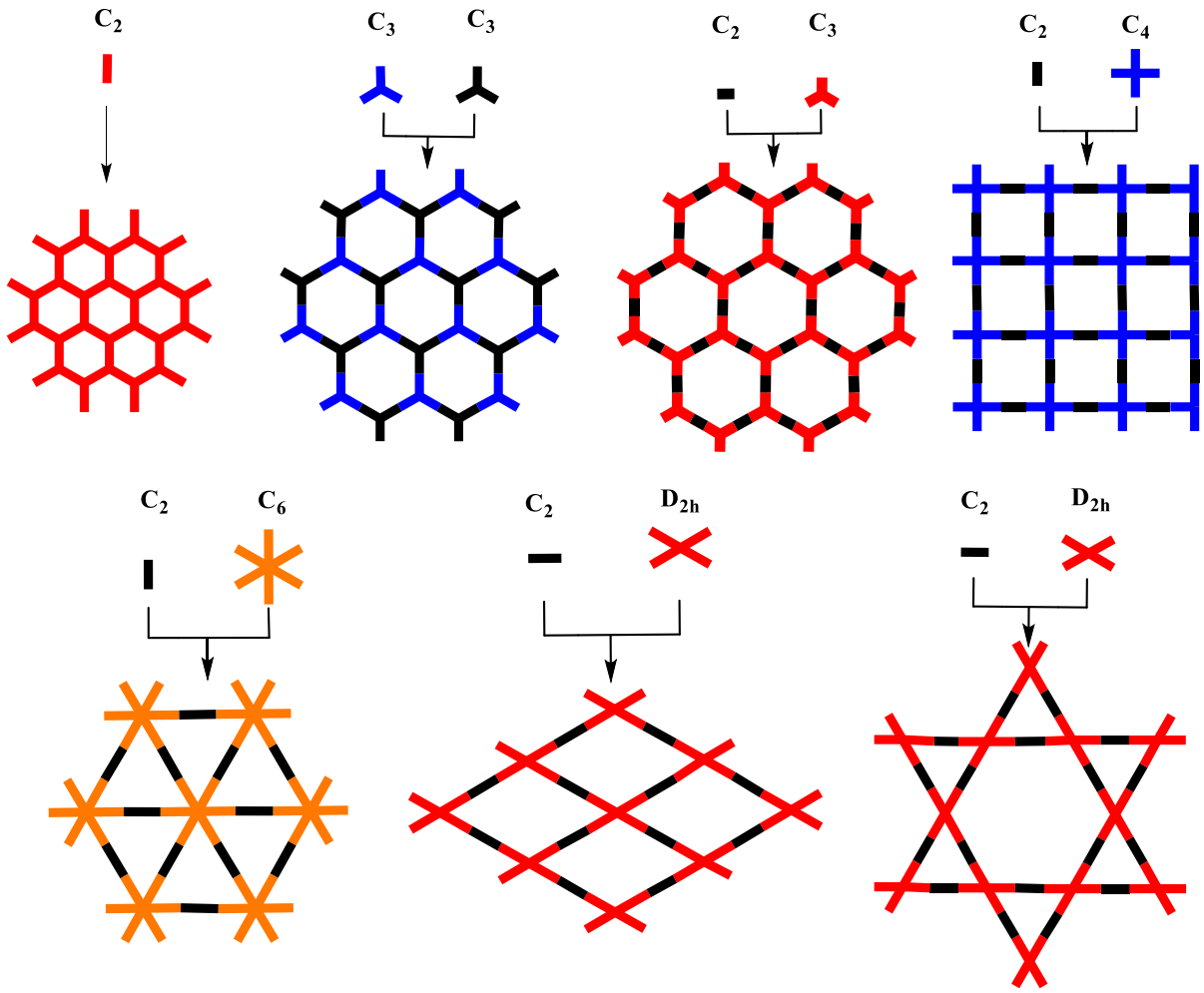

Figure 4. Various types of topological diagrams for the design of 2D COFs. Redrawn from reference[9]

Boroxine acids are self-condensed and make a planar rigid structure with a six-member ring and water as a side product. The variant of boroxine-linked COFs like PPy-COF and 2D COF-1 were constructed from the reaction between different chromophores of diboronic acids such as pyrene-2,7-diboronic acid and 1,4-benezenediboronic acid. The reaction between catechol derivatives and boronic acids forms boronate-ester linkage, which has a cyclic rigid five-membered ring and a planar structure. Examples of 2D crystalline COFs are COF-8, TT-COF, COF-6, H_2P-COF, TP-COF, COF-10, and COF-66. In the same fashion, 3D crystalline COFs such as DBA-3D-COF-1, COF-105, and COF-108 have been synthesized by taking different monomers that possess T_d geometry. Boronate-ester linkage, a five-member ring, builds high crystalline COFs due to its reversibility and highly rigid planar structure.

A Schiff base reaction between an aldehyde and aromatic amine with Lewis acid or organic acid catalyst can produce imine linkage. The imine-linked 2D COFs could be divided

into five types such as rhombic, hexagonal, kagome, square, and tetragonal architecture, based on their topology diagram.[23] Several solvents have been applied to the solvothermal reactions at different temperature conditions and times, including ethanol, *o*-DCB/n-butanol, THF/methylene, and DMAc/*o*-DCB. The appropriate monomer as TAA and TAPM might be acting as a node for 3D crystalline COFs. A hydrazone is linked to building by the derivative of hydrazide and aldehyde monomers in the presence of Lewis acid catalyst as acetic acid.

The C=C bonded COFs are entirely π-conjugated and could be attained via a Knoevenagel condensation reaction between derivatives of benzyl cyanides and aldehydes in the presence of sodium hydroxide, potassium hydroxide, and different kinds of secondary amine bases. These bases act as a catalyst in this condensation reaction. The earliest C=C bonded crystalline COFs are g-C37N3-COF and g-C40N3-COF. Each crystalline COFs can be synthesized in the presence of DMF solvent with the help of a base catalyst as piperidine at a very high temperature. Other than this linkage, amide linkage, 1,4-dioxane linkage, urea linkage, viologen linkage, spiroborate linkage, phenazine linkage, and squaraine linkage are used for building COFs. A stable COF formation occurs when phenazine linkage is present in COF where fused planar rigid structure and π-conjugation give this framework high stability. In solvothermal conditions, tert-butylpyrene tetraone and triphenylene hexamine monomers react with each other and form phenazine-linked COFs.

Generally, CTFs created by the ring formation reaction by 1,4-benzonitrile in the presence of white crystalline $ZnCl_2$ at a very high temperature around 450 °C – 600 °C. The diversity of CTFs is very narrow and is proportionally less crystalline than COFs building blocks.

1.5 Synthetic Methods

There are various methods from which porous material can be synthesized. Many research groups have diversified synthetic methods that are majorly being used, consisting of solvothermal, ionothermal, microwave, room temperature, and light promoted methods.[24]

1.5.1 Solvothermal Synthesis

In general, the solvothermal method is a well-known method for synthesizing porous organic material. In this method, the mixture of different symmetries, an organic building block for node and vertices, polar/nonpolar solvent combination in different proportions, and the catalyst all are mixed in a tube. After that, this reaction mixture is sonicated for a few

minutes, degassing for three-four freeze-pump-thaw cycles, sealing that tube with the flame, and

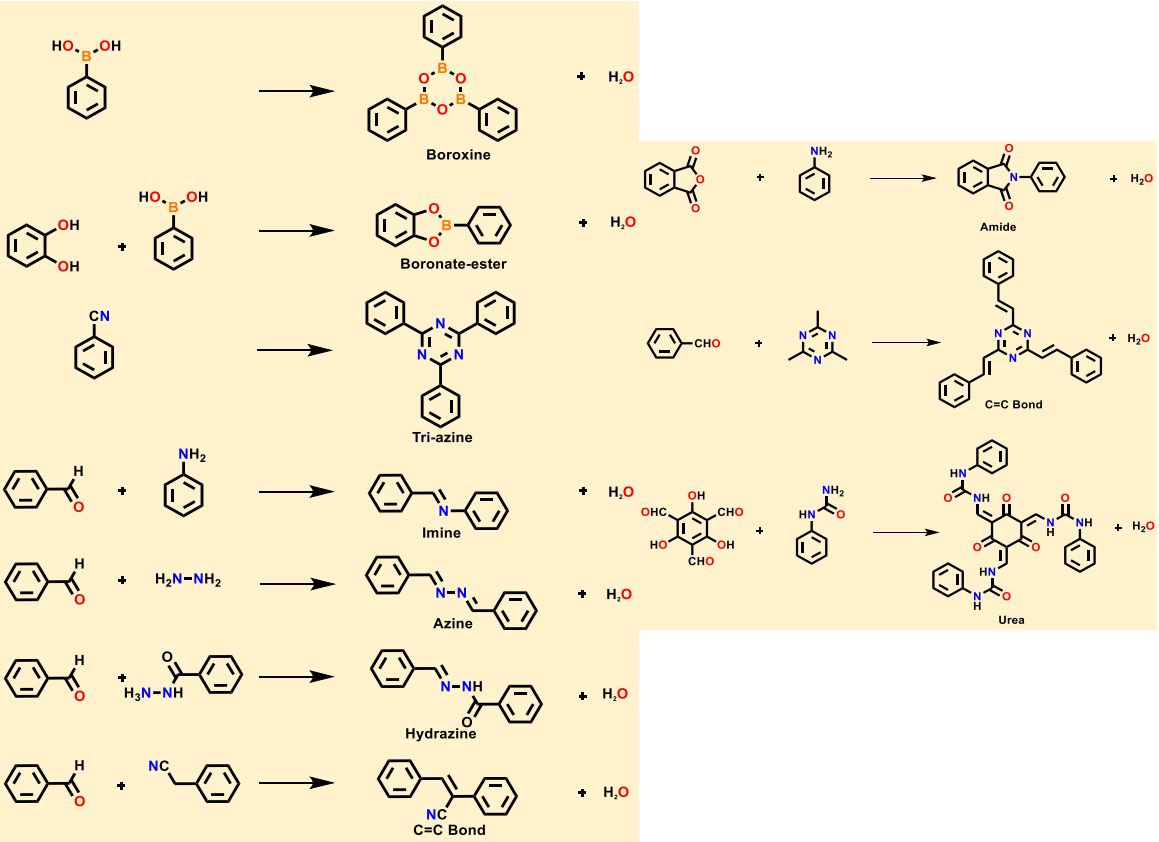

Figure 5. Various types of condensation reactions for the formation of COFs. Redrawn from reference[7]

keep that reaction mixture at a high temperature for three-four days. After three-four days, that tube must be cooled to room temperature, and the precipitation separated by centrifuging or filtering the reaction mixture and cleaned with various solvents. The filtrate is preserved under a vacuum at 100 °C – 120 °C and stored in an argon or nitrogen atmosphere.[25]

1.5.2 Microwave Synthesis

Compared to the prolonged reaction times required by solvothermal procedures, the microwave synthetic method is used as the efficient synthesis of crystalline porous organic polymer. By using this synthetic method, different kinds of linkages were synthesized such as COF-102 and COF-5, boronate linkage, and TpPa-COF, an imine-linked COF successfully.[26]

1.5.3 Mechanochemical Synthesis

The exploratory simple synthetic approach is desirable since microwave, and solvothermal synthesis operations are done under harsh conditions (e.g., a reaction in a closed Pyrex tube, certain solvents, an inert environment, and a very high temperature for

crystallizing this powder). In this method, monomers are in a mortar, crushed with a grinder at ambient room temperature. For example, TpBD-Me_2, TpPa-2, TpPa-NO_2, and TpBD were synthesized by taking the help of this method.[27] A negligible amount of catalyst is added during suitable grinding monomers.

1.5.4 Ionothermal Synthesis

Most of the CTFs are amorphous materials and have a deficit of rigid, planar, and prolonged range of molecular orderings. However, many CTFs produced under ionothermal conditions, such as CTF-2 and CTF-1 are examples of crystalline porous frameworks. The general method of this porous material is that white crystalline $ZnCl_2$ and monomer were taken in a tube, removed air, sealed, and heated to 400 ºC for two days. The mixture is kept at room temperature for cooling. After that, grind that reaction mixture and continuously clean it with water to take out $ZnCl_2$. Due to a different type of impurity in the reaction mixture, the final powder was put into a beaker with HCl solution and swirled for at least 24 hours to remove $ZnCl_2$. Then filtered, the reaction mixture and washed with different solvents like water, DCM, and THF. At last, dried the final crude product was under vacuum to obtain CTFs. The reversibility of this condensation reaction is due to the molten salt functions of $ZnCl_2$, which acts as a solvent and a catalyst in this high-temperature reaction.[28]

1.6 Application

COFs are a unique category in porous organic materials because of their everlasting porosity, high surface area, regular pore channel, high thermal and chemical stability, and organic building block. Due to these properties, COFs can be used in a vast area of applications. This section briefly addresses some of the uses in the area (for example- energy conservation, catalysis, gas adsorption and storage, semiconduction, photocatalysis, and drug delivery).[29-33]

Our universe is abundant in diverse energy resources, including sunshine, nuclear energy, fossil fuels, hydro, and geothermal, all of which are converted into electricity via appropriate technologies, providing a non-stop source of power for civilization and modernization of daily activities. This topic, energy storage, and conversion is a fundamental topic that is especially vital to long-period growth. Over the last years, organic materials for devices and storing electricity have achieved symbolic advances in our daily lives. COFs can have redox-active skeletons, discrete pores, and unique walls. These features are essential in

electrochemical processes involving energy storage. The unique redox-active structures encourage energy separation and storage, and the pores allow for ion transport and storage.[34] Predesigning porous organic materials are valuable for energy devices, semiconductors, and optoelectronics by taking the help of hole, electron, and ions transport. The unique design of 2D/3D COFs gives rise to the integral structure of 1D open pores and skeletons of the framework that can accommodate specific molecular and ionic guests.

COFs can be designed by analyzing pore-surface engineering and diagrams of topology, which could serve as a scaffolding for molecular gas separation and adsorption. Porosity, very high surface area, and low density are requirements for different kinds of gas separation and adsorption. Over the last few years, 2D COFs can be beneficial for hydrogen adsorption, methane adsorption, gas separation, chiral compound separation, depending on their structural designability and diversity.[35]

COFs provide a well-defined platform for coordinating metals, with open reactive sites and adjustable bandgaps between VB and CB. COFs are also attractive catalyst options for photocatalytic and electrocatalytic systems due to their porosity and tunability of resultant structure with a very high surface area. COFs possess well-defined pores, structures, and reactive organic linkers are essential features in considering the catalytic sites. The targeted catalytic sites depended on the predesigned catalytic site of the framework. Due to their adequate stability and reusability, organic semiconducting materials with acceptable bandgaps are among the most intensively investigated heterogeneous photocatalysts. As a result, one essential characteristic is that the organic dye-based porous material catalysts may be energized for cycle usage after a simple separation from the reaction mixture following filtering of the reaction mixture or centrifugation. COFs can perform photocatalysis, electrocatalysis, oxygen evolution reactions, chiral catalysis, reduction of carbon dioxide reactions, etc.[36]

After post-synthetic modification, COFs could utilize as drug delivery vectors for typical deficiency of chemical stability and functionality. The time-consuming synthetic hurdle and undesirable metal ions that have leached from the carriers are poisonous and may result in poor drug delivery efficacy. Post-synthetic alteration is an effective way to give COFs drug-delivery capabilities.[27]

Chapter 2

2.1 Objective

Covalent organic frameworks (COFs) are excellent heterogeneous photocatalysts due to their insolubility in all organic solvents and recyclability during photocatalytic conversion. All inorganic semiconducting materials still show decisive deficiencies, such as rapid charge recombination, operation in the UV region, low efficiency, etc. A classical photocatalyst should satisfy several requirements, such as following a wide range of visible light areas, a well-organized band gap framework, and charge transfer and separation to achieve symbolic efficiency in heterogeneous photocatalytic activity. Heterogeneous photocatalysts are made of metal-free organic semiconductor materials, such as CMPs and carbon nitrides.[37] Under visible light, COFs can act as heterogeneous photocatalysts for photocatalytic CO_2 reduction, H_2 evolution, and synthetic organic transformation reactions. COFs provide a well-defined framework for coordinating metals, with adjustable bandgaps and open sites. COFs are also attractive catalyst options for photocatalytic and electrocatalytic systems to their porosity and structural tunability with high surface area.

The focus of this study is to synthesize a low bandgap COF that can be used as a heterogeneous catalyst. For this purpose, monomers, TAPT, and BTD were mixed in the presence of 6 M acetic acid, resulting in TAPT-BTD-COF, under solvothermal conditions. TAPT-BTD-COF was used as a heterogeneous, recyclable photocatalyst to convert para-substituted benzaldehyde to an imidazole ring in mild conditions.[38,39] Visible light and room temperature are preferred conditions. Compared to traditional metal-based photocatalysis, an ecologically benign metal-free approach is more likely for society.

2.2 Materials and Method

The solvents and chemicals were used as received without further purification. Thin-layer chromatography (TLC) was carried out on an aluminum sheet precoated with silica gel (Merck, Kieselgel 60, F254). Column chromatography was carried out on silica gel (60-120 and 100-200 mesh). The structural characterizations of the synthesized compounds were investigated by ^{1}H NMR and ^{13}C NMR (Bruker Biospin Switzerland Avance-iii 400 MHz and 100 MHz spectrometers, respectively) and Fourier Transform Infrared (FT-IR) spectroscopy (Perkin Elmer Spectrum Two), Powder X-ray diffraction (PXRD) (GeniX 3D,

Xenocs), Thermogravimetric analysis (TGA) (Shimadzu DTG-60), Surface Area Measurements (Quantachrome ASiQwin automatic) and UV-vis Measurements (Agilent Technologies, Cary 5000). For intermediate and final compounds, FT-IR was performed as KBr pellets. Deuterated solvents such as $CDCl_3$ and DMSO-d_6, as well as tetramethylsilane (TMS) as an internal standard, were used to record ^{1}H and ^{13}C NMR spectra.

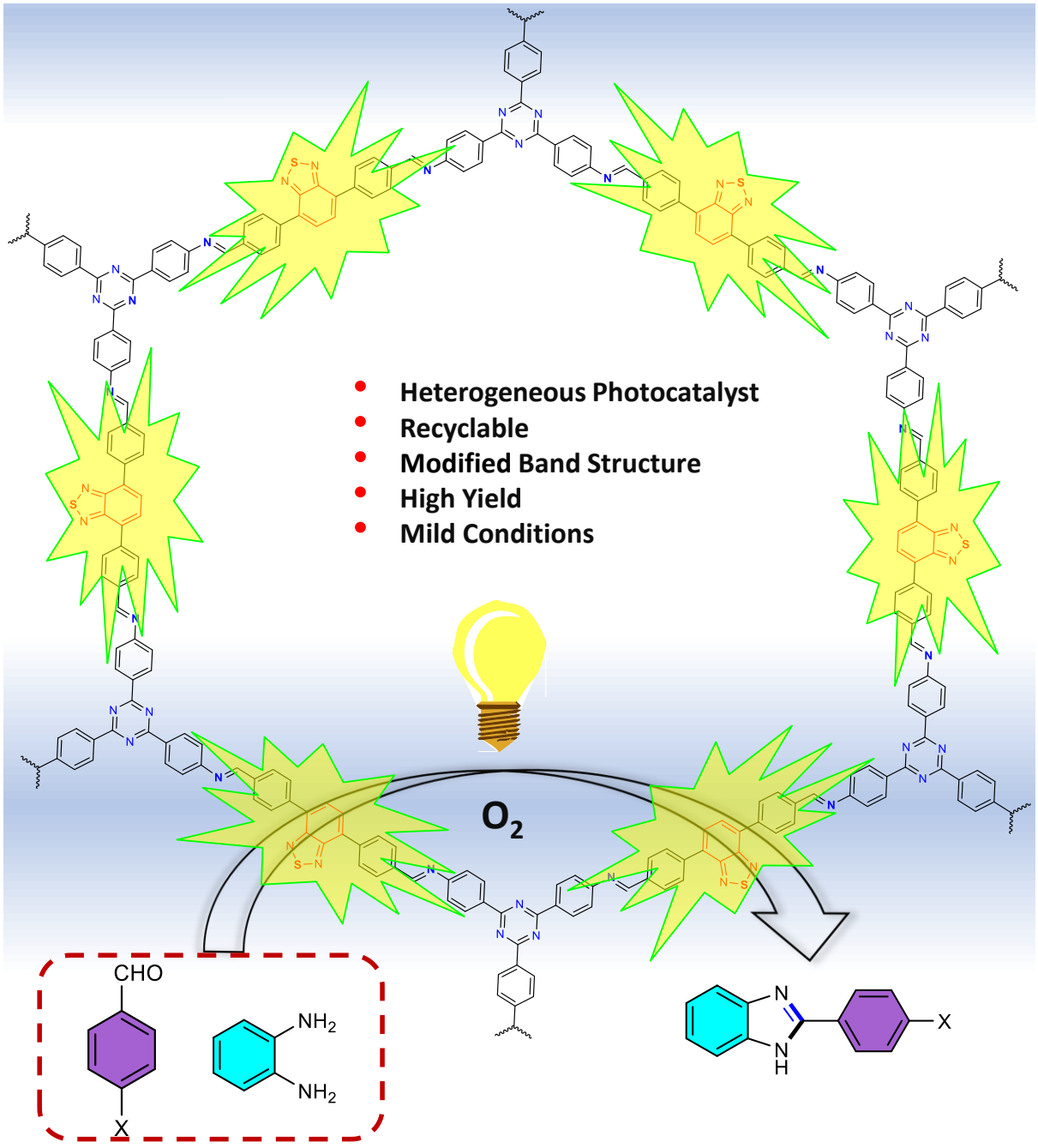

Figure 6. Heterogeneous photocatalytic application of TAPT-BTD-COF.

2.3 Synthesis of Monomers and COFs

2.3.1 Synthesis of 1,3,5-tris-(4-aminophenyl)triazine (TAPT)

TAPT was synthesized according to the previously reported method.[40] A two-neck round-bottom flask was filled with 4-aminobenzonitrile (350 mg, 6.54 mmol). Then, in an inert environment at zero temperature, trifluoromethanesulfonic acid (2 mL, 44.4 mmol) was added slowly drop by drop. The reaction mixture was stirred for 24 h at room temperature under normal circumstances. For this experiment, we added distilled water into the final reaction mixture and aqueous sodium hydroxide solution to neutralize it until the pH was around 7. After then, that reaction mixture was extracted with ethyl acetate(EtOAc) (50 mL). The organic phase and water phase separated, then the organic phase dried with the help of $MgSO_4$. The solvent was removed by a reduced pressure evaporator. The pale-yellow solid was purified with 60-120 mesh silica gel column chromatography (petroleum: ethyl acetate = 1:1)—yielding around 55%. ^{1}H NMR (400 MHz, DMSO-d_6): δ (ppm): 8.34 (d, J = 8.6 Hz, 6H), 6.70 (d, J = 8.68 Hz, 6H), 5.92 (s, 6H). ^{13}C NMR (100 MHz, DMSO-d_6): δ (ppm): 170.02, 153.44, 130.61, 123.36, 113.56.

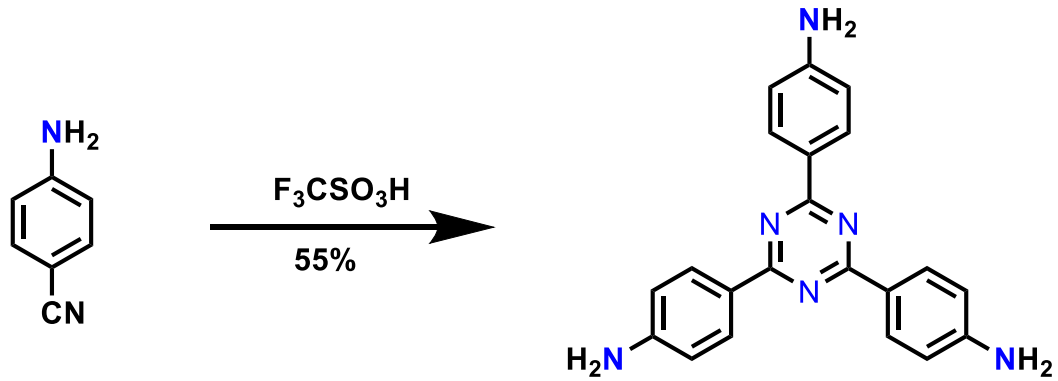

Scheme 1. Synthetic scheme of TAPT.

2.3.2 Synthesis of di-(benzothiadiazole-4,7-diyl)Di-benzaldehyde (BTD)

TAPT was synthesized using a slightly different version of a previously published technique.[41] The mixture of 4,7-dibromo-2,1,3-benzothiadiazole (0.59 g, 2.0 mmol), 4-formyl phenylboronic acid (1.18 g, 8.0 mmol), Caesium Carbonate (1.3 g, 8mmol), and tetrakis(triphenylphosphine) palladium (0.12 g, 1.0 mmol) were taken in two neck round

bottom flask. We put the reaction mixture for inert conditions. After then, the solvent mixture of toluene and ethanol was added to the reaction mixture under inert conditions. After adding solvent to the reaction mixture, we put the reaction mixture at 90 °C for 42 h. This reaction mixture was followed by extracting the crude product with dichloromethane. The organic phase and water phase separated and the organic phase dried with the help of $MgSO_4$. A reduced pressure evaporator removed the solvent. The yellow residue was refined with silica gel column chromatography (hexane: ethyl acetate = 4:1)—yielding around 70%. ^{1}H NMR (400 MHz, $CDCl_3$): δ (ppm): 10.13 (s, 2H, -CHO), 8.17 (d, J = 8.0 Hz, 4H, Ar-H), 8.09 (d, J = 8.0 Hz, 4H, Ar-H), 7.91 (s, 2H, Ar-H). ^{13}C NMR (100 MHz, $CDCl_3$): δ (ppm): 191.87, 142.95, 136.05, 133.01, 130.02, 128.71.

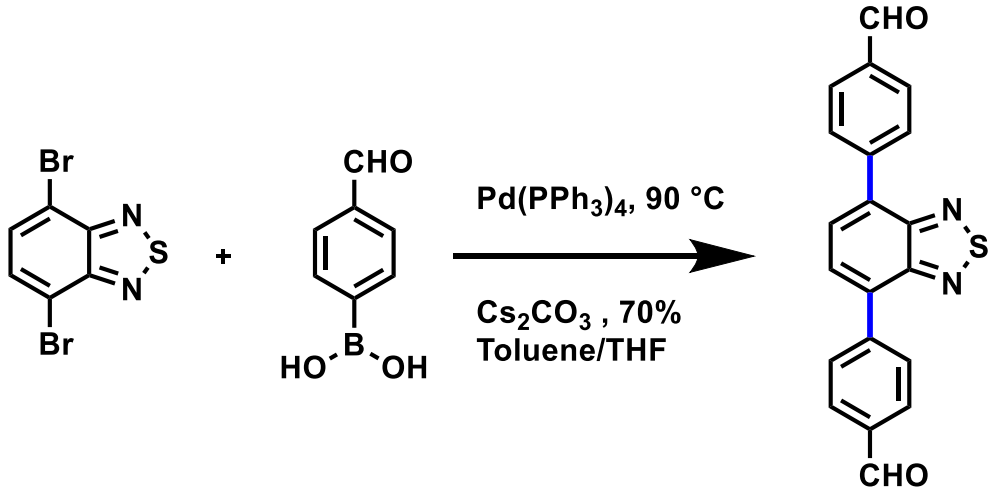

Scheme 2. Synthetic scheme of BTD-CHO.

2.3.3 Synthesis of TAPT-BTD-COF

TAPT, BTD-CHO and mesitylene/dioxane (4:1 v/v, 1 ml) were charged into a 5 mL glass tube. This resultant mixture was then sonicated for 3-5 min., resulting in a yellowish-orange precipitate in the solution. 0.1 mL of acetic acid (6M) was eventually added to this reaction mixture. After that, the reaction mixture was sonicated for a second time for 5 min. After that, the tube was flash-frozen with a liquid nitrogen bath at 77 K, degassed with freeze-pump-thaw for three cycles, vacuum-sealed, and heated for 72 h. at 120 °C. The obtained precipitate was then washed 3-4 times using various solvents such as N, N-dimethylformamide, anhydrous ethanol, acetone, and dichloromethane. The recovered substance was vacuum dried for 24 h, yielding a yellowish-orange powder.

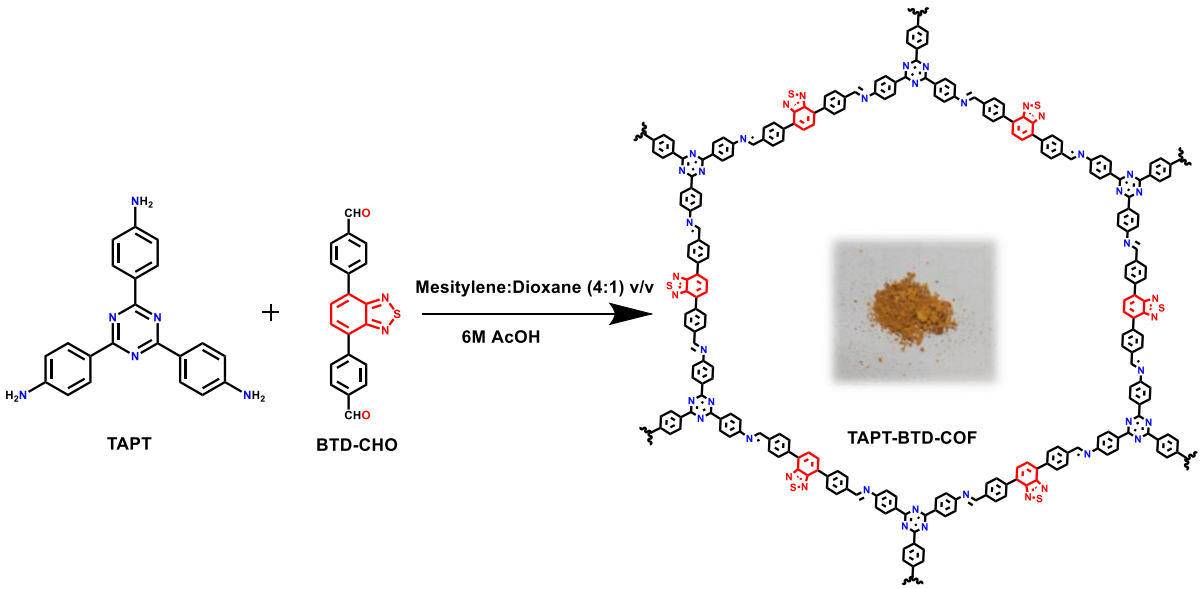

Scheme 3. Synthetic scheme of TAPT-BTD-COF.

2.4 Bulk Characterization of TAPT-BTD-COF

The successful formation of TAPT-BTD-COF was initially characterized by FT-IR spectroscopy. A powder X-ray diffraction (PXRD) study was used to understand the crystallinity of TAPT-BTD-COF. Measurement of surface area and pore diameter were characterized by nitrogen adsorption-desorption isotherm. Thermal stability was characterized by thermogravimetric analysis (TGA). In this section, the observed results from these studies are discussed in detail.

2.4.1 FT-IR Spectroscopy:

The FT-IR spectra of TAPT, BTD-CHO, and TAPT-BTD-COF are given in Figure 7. The carbonyl stretching (C=O) frequency of BTD-CHO at 1696 cm^{-1} and amine (N-H) stretching frequency in TAPT at 3320 cm^{-1} disappeared from spectra of TAPT-BTD-COF. A new stretching frequency at 1571 cm^{-1} appeared in the FT-IR spectrum of TAPT-BTD-COF that could be assigned as imine (C=N) stretching vibrations.

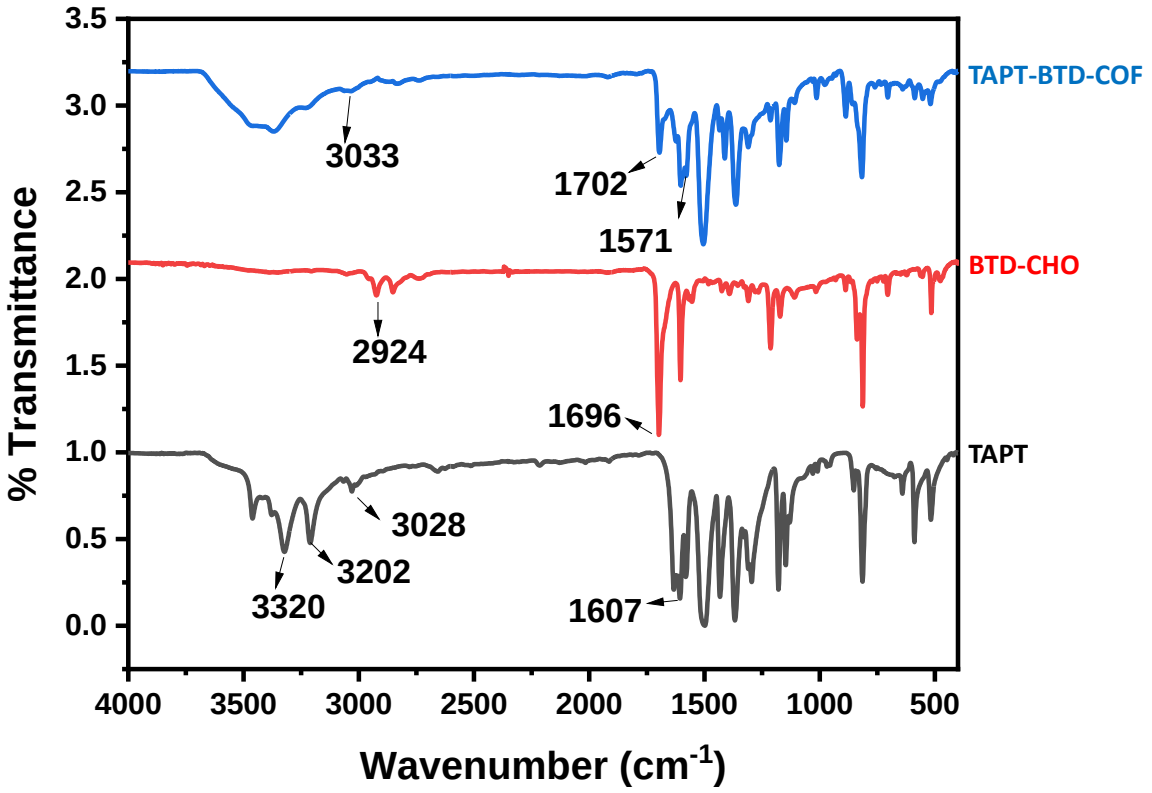

Figure 7. FT-IR spectra of TAPT (black), BTD-CHO (red), and TAPT-BTD-COF (blue).

2.4.2 Powder X-ray Diffraction (PXRD) pattern of TAPT-BTD-COF:

The powder X-ray diffraction (PXRD) was used to analyze the crystallinity of TAPT-BTD-COF. As shown in Figure 8, the first prominent peak was observed at 3.6°. Several other weak reflections were also observed at 4.9°, 6.3°, and 19.0°. The broad peak at 19.0° could be assigned to the π - π stacking between layers TAPT-BTD-COF.

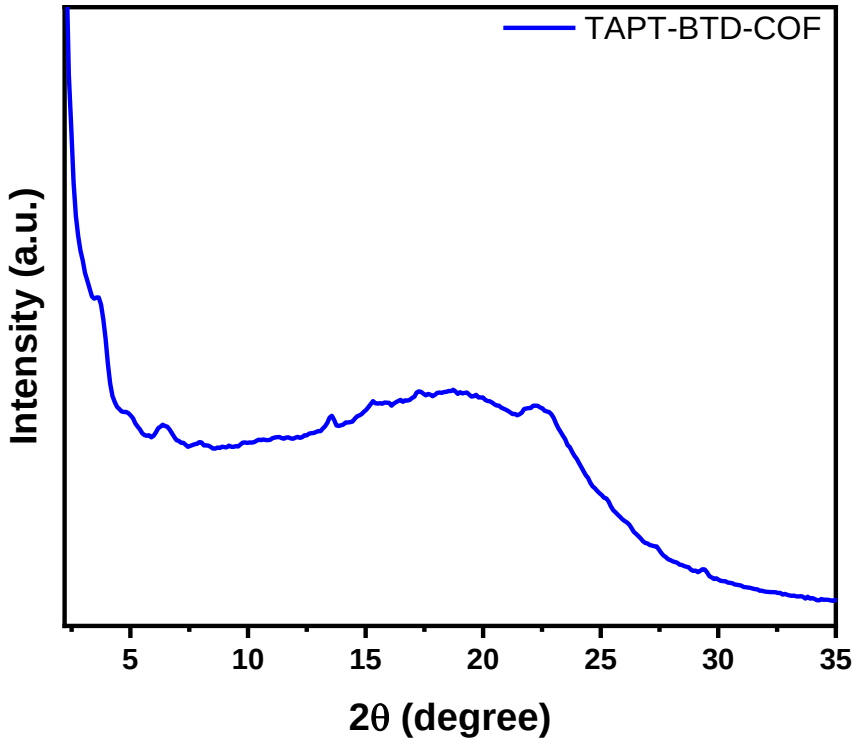

Figure 8. Powder X-ray diffraction (PXRD) pattern of TAPT-BTD-COF.

2.4.3 Brunauer–Emmett–Teller (BET):

Nitrogen sorption measurements at 77 K showed the formation of micropores in the low relative pressure region. The type IV adsorption-desorption isotherms suggested the mesoporous nature of TAPT-BTD-COF. Brunauer–Emmett–Teller (BET) surface area was calculated to be 329 m^2 g^{-1}. Non-local density functional theory (NLDFT) was used to measure the pore size distribution (PSD), which showed a prominent peak with a pore radius of 2.6 nm. (Figure 9).

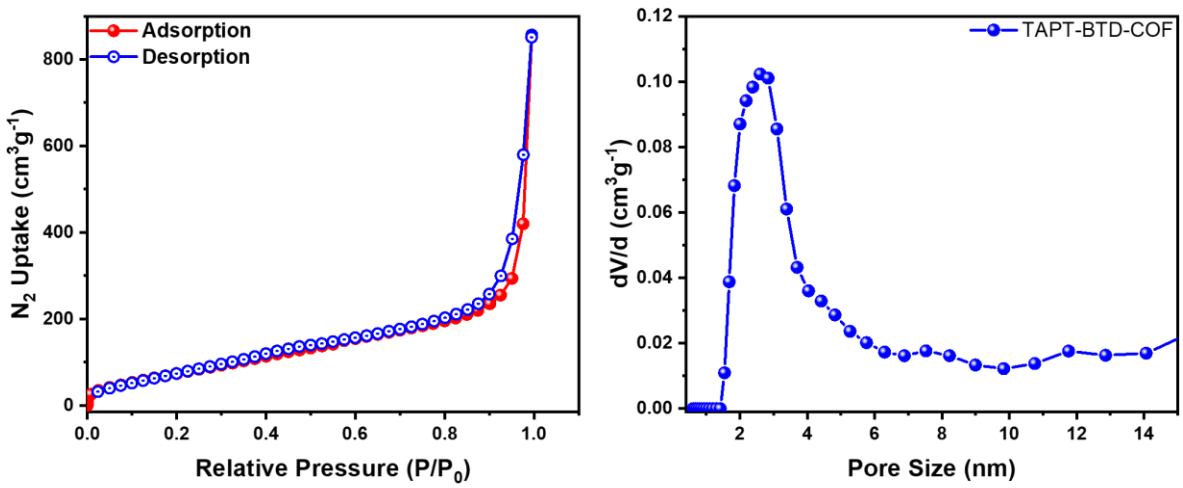

Figure 9. N_2 adsorption-desorption and pore size distribution curve of TAPT-BTD-COF.

2.4.4 Thermogravimetric Analysis (TGA):

Thermogravimetric analysis displayed that the TAPT-BTD-COF is stable up to 440 °C, as shown in Figure 10.

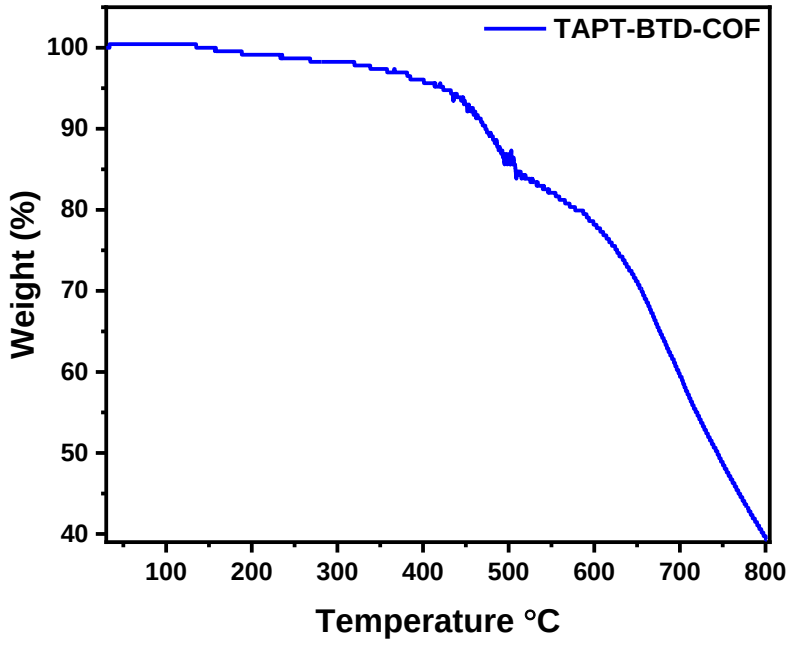

Figure 10. TGA plot of TAPT-BTD-COF.

2.4.5 UV-vis spectroscopy

UV-vis spectra of TAPT-BTD-COF showed a broad light absorption with maximum absorption at 492 nm, as shown in Figure 11.

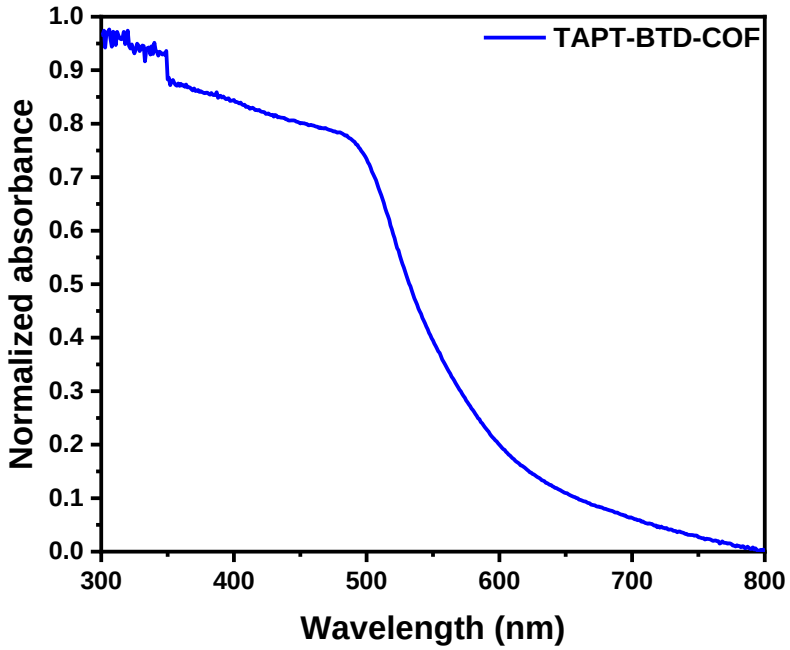

Figure 11. UV-vis spectra of TAPT-BTD-COF.

2.5 Application of TAPT-BTD-COF

TAPT-BTD-COF possesses inherent porosity, high stability, well-defined photo redox characteristics, and a significant UV harvesting material. Those characteristics are met in theory for well-defined heterogeneous photocatalysts. As a consequence, to discover the optimum photocatalyst from this TAPT-BTD-COF, we employed benzimidazole photosynthesis as a model reaction. The photocatalytic activity of new COFs for the formation of benzimidazole in the presence of visible light was also investigated, using o-phenylenediamine, benzaldehyde, and molecular oxygen as starting materials. But, without TAPT-BTD-COF and no visible light, this coupling would not be facile to produce an imidazole ring.[38] Here, benzothiadiazole, which can be used as a photocatalytic dye, employs to narrow the gap between the valance and conduction bands. The obtained TAPT-BTD-COF was used here as a photocatalyst for oxidative coupling between o-phenylenediamine and aromatic aldehyde.

2.5.1 Oxidative coupling reaction between o-phenylenediamine and aromatic aldehyde

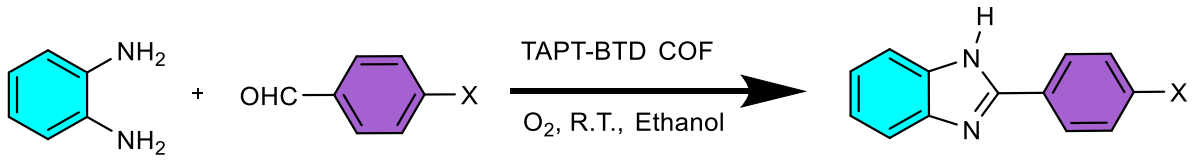

Scheme 4. Synthetic scheme of the oxidative coupling reaction between o-phenylenediamine and aromatic aldehyde.

Table 1: Optimization of the conditions for visible-light-driven oxidative coupling reaction between o-phenylenediamine and aromatic aldehyde.

Substrate	Solvent	Catalyst	Yield	Time
1	Ethanol	TAPT-BTD-COF	96%	2h
2	Ethanol	TAPT-BTD-COF	94%	2h
3	Ethanol	TAPT-BTD-COF	87%	2h
4	Ethanol	TAPT-BTD-COF	83%	2h
5	Ethanol	No Catalyst	~	2h
6	Ethanol	No Catalyst, No Light	~	2h

Table 2: Photocatalytic oxidative coupling of various aromatic aldehyde by TAPT-BTD-COF.

Entry	Substrate	Product	Time(h)	Conv. (%)
1	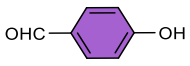	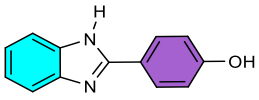	2h	96%
2	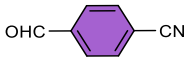	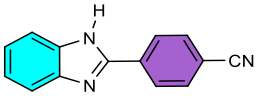	2h	94%
3	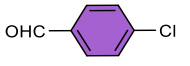	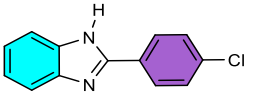	2h	87%
4	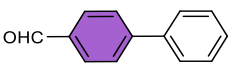	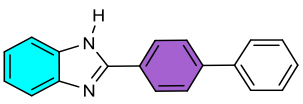	2h	83%

Appendices

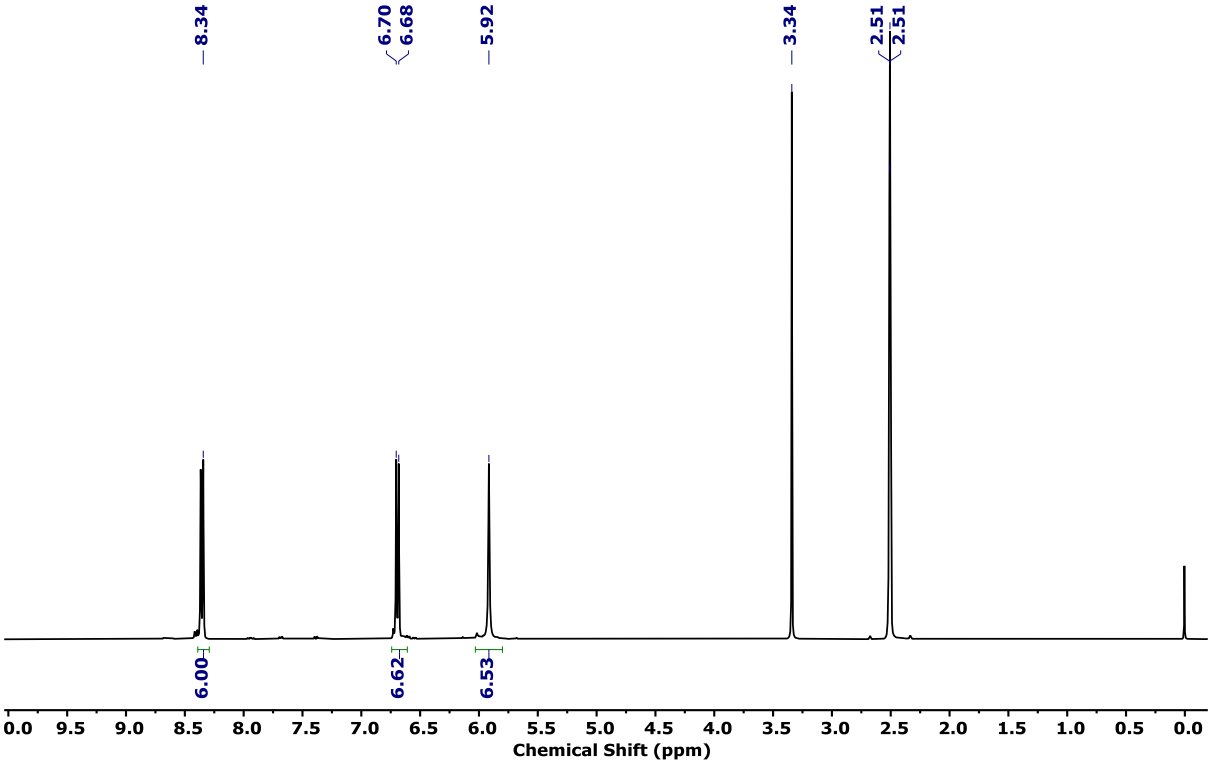

Figure 12. The ^{1}H NMR (400 MHz, DMSO-d_6) of 1,3,5-tris-(4-aminophenyl)triazine.

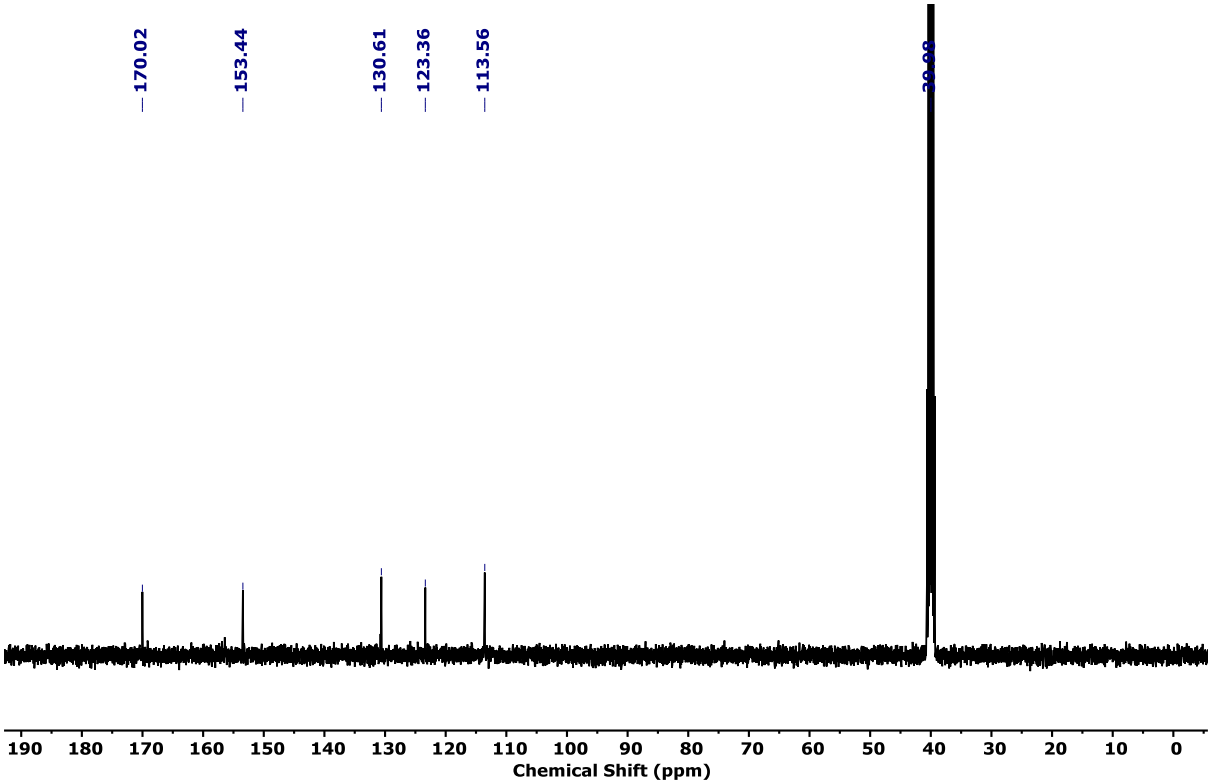

Figure 13. The ^{13}C NMR (100 MHz, DMSO-d_6) of 1,3,5-tris-(4-aminophenyl)triazine.

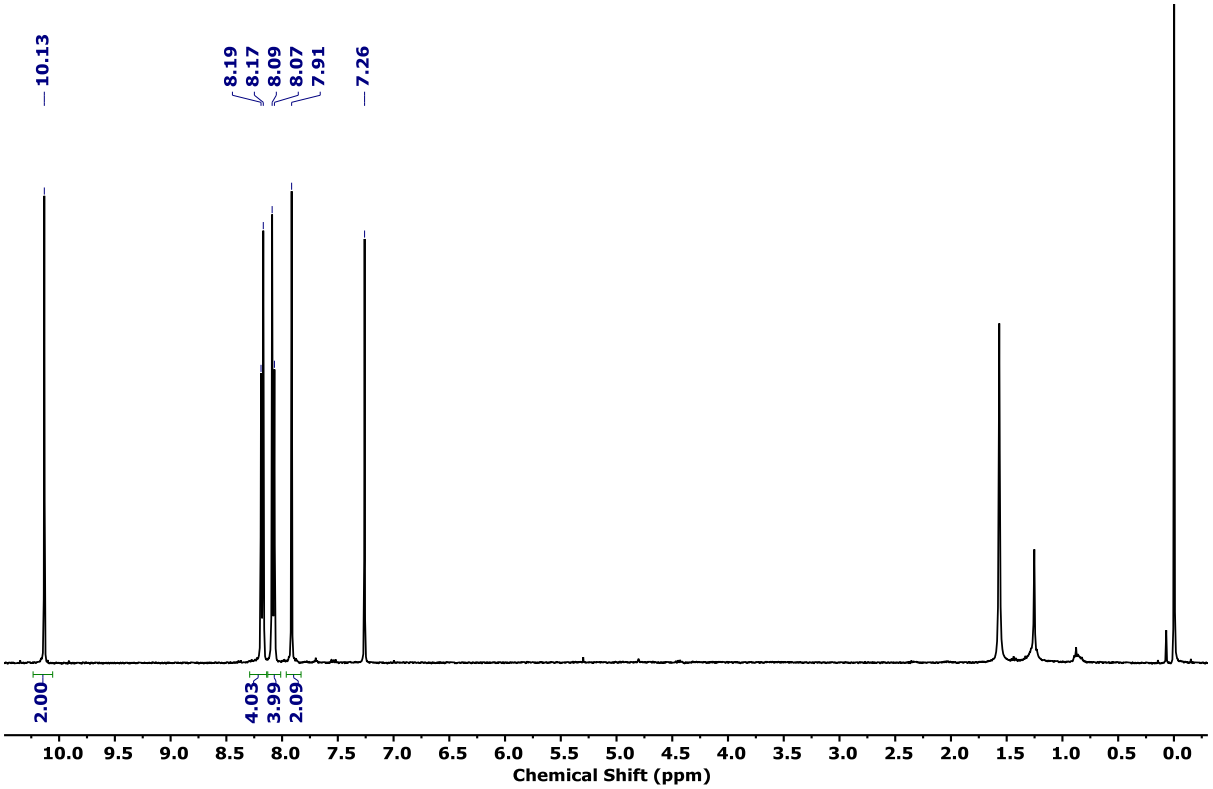

Figure 14. The ^{1}H NMR (400 MHz, $CDCl_3$) of di-(benzothiadiazole-4,7-diyl)Di-benzaldehyde.

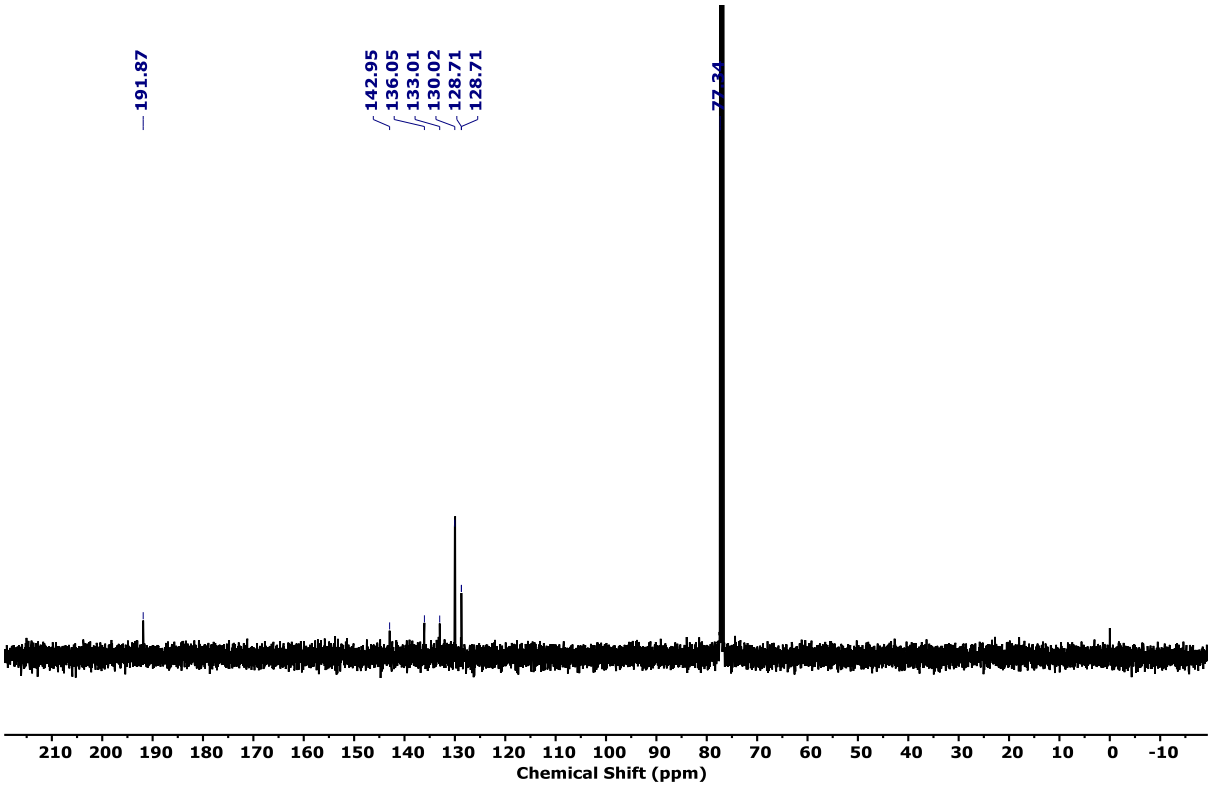

Figure 15. The ^{13}C NMR (100 MHz, $CDCl_3$) of di-(benzothiadiazole-4,7-diyl)Di-benzaldehyde.

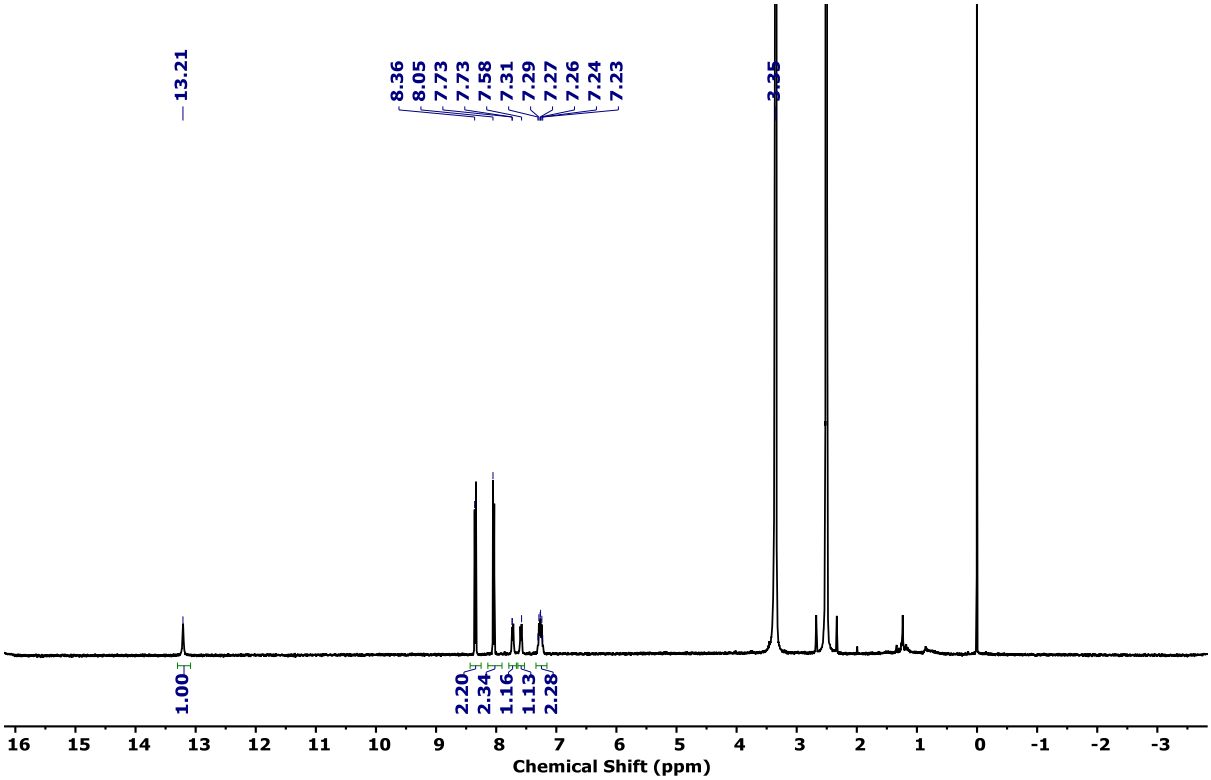

Figure 16. The ^{1}H NMR (400 MHz, DMSO-d_6) of 4-(1H-benzo[d]imidazol-2-yl)benzonitrile (A).

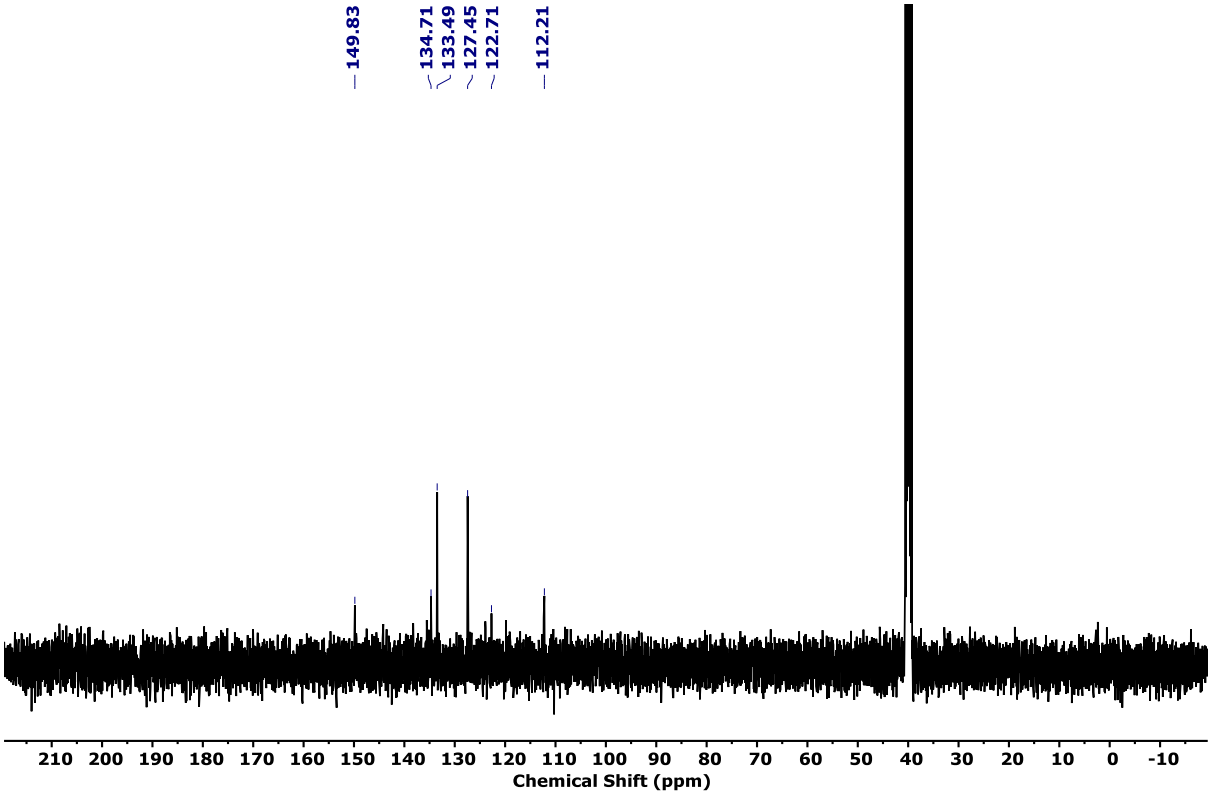

Figure 17. The ^{13}C NMR (100 MHz, DMSO-d_6) of 4-(1H-benzo[d]imidazol-2-yl)benzonitrile (A).

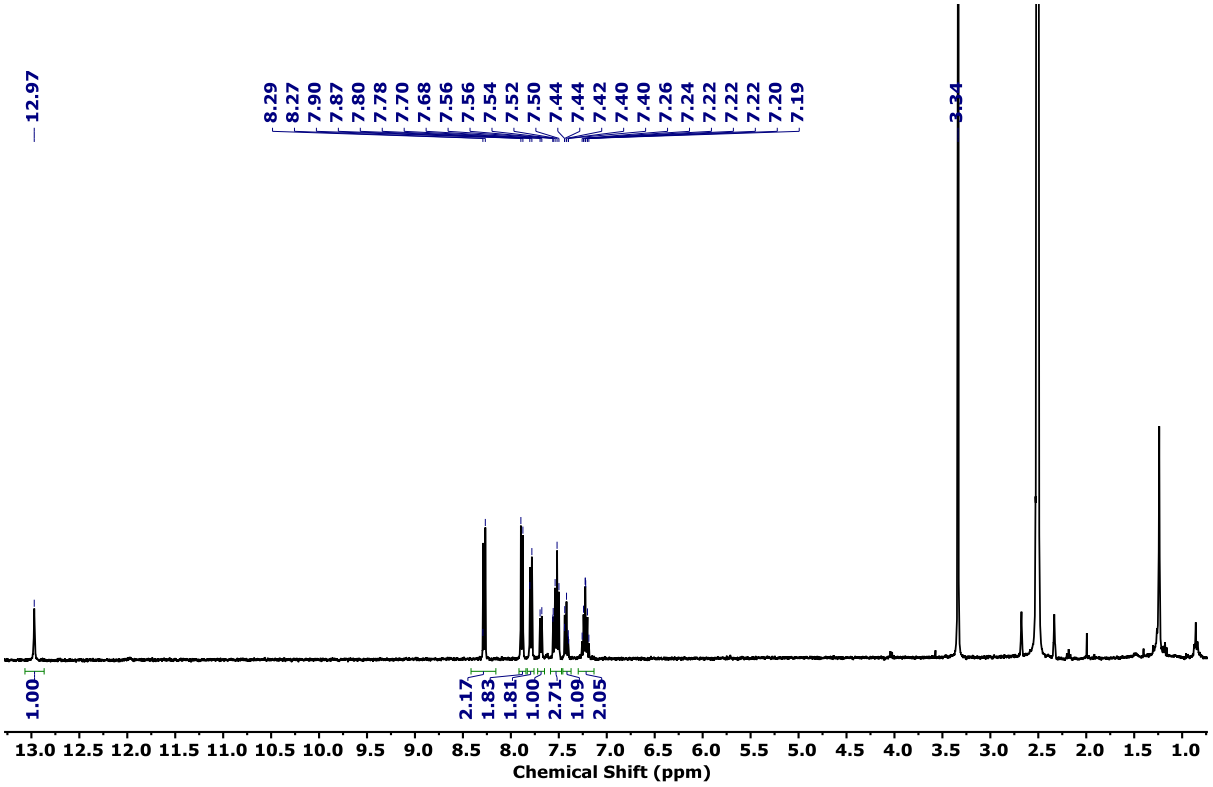

Figure 18. The ^{1}H NMR (400 MHz, DMSO-d_6) of 2-([1,1'-biphenyl]-4-yl)-1H-benzo[d]imidazole (B).

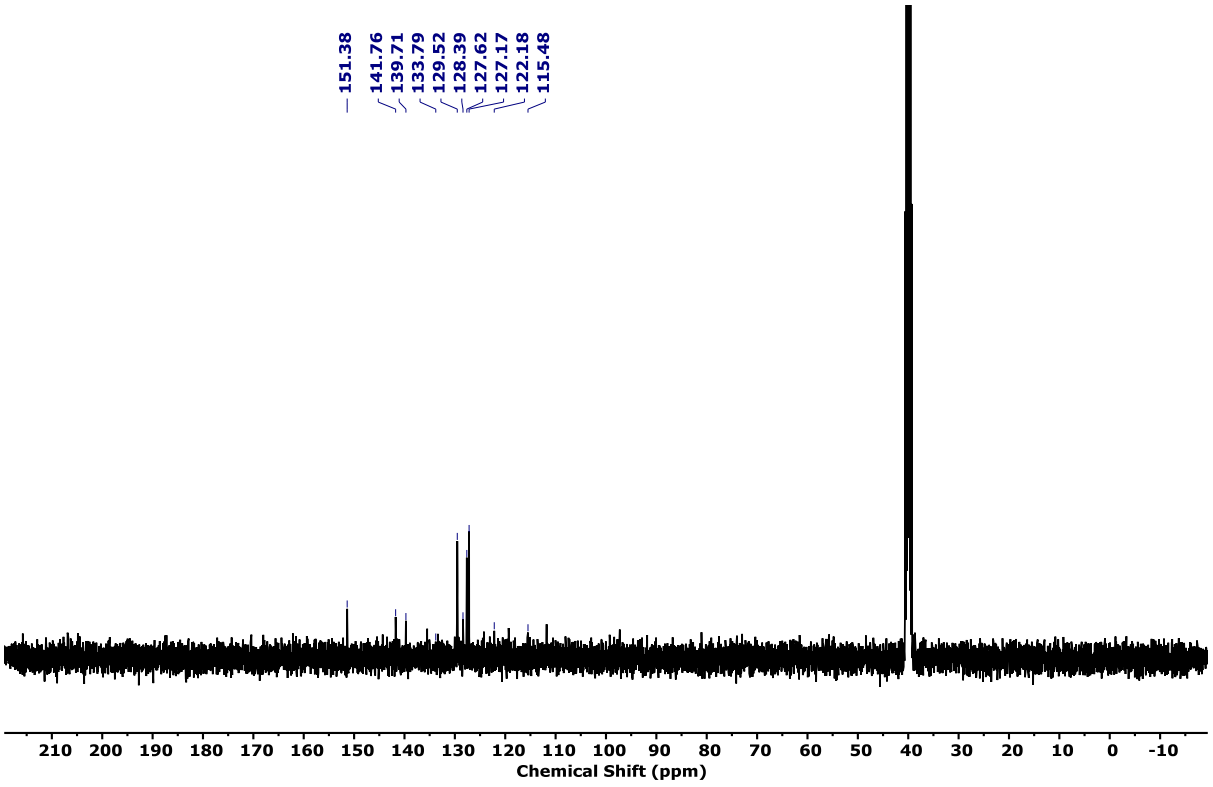

Figure 19. The ^{13}C NMR (100 MHz, DMSO-d_6) of 2-([1,1'-biphenyl]-4-yl)-1H-benzo[d]imidazole (B).

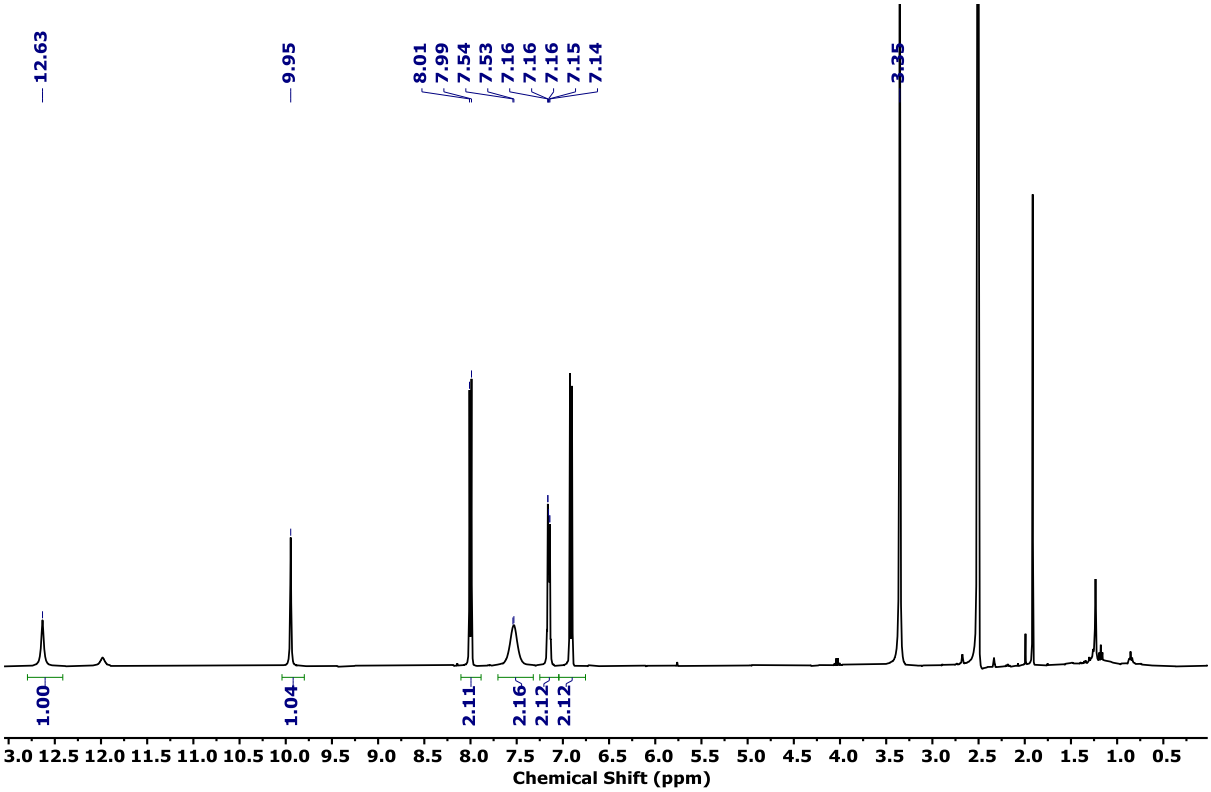

Figure 20. The ^{1}H NMR (400 MHz, DMSO-d_6) of 4-(1H-benzo[d]imidazol-2-yl)phenol (C).

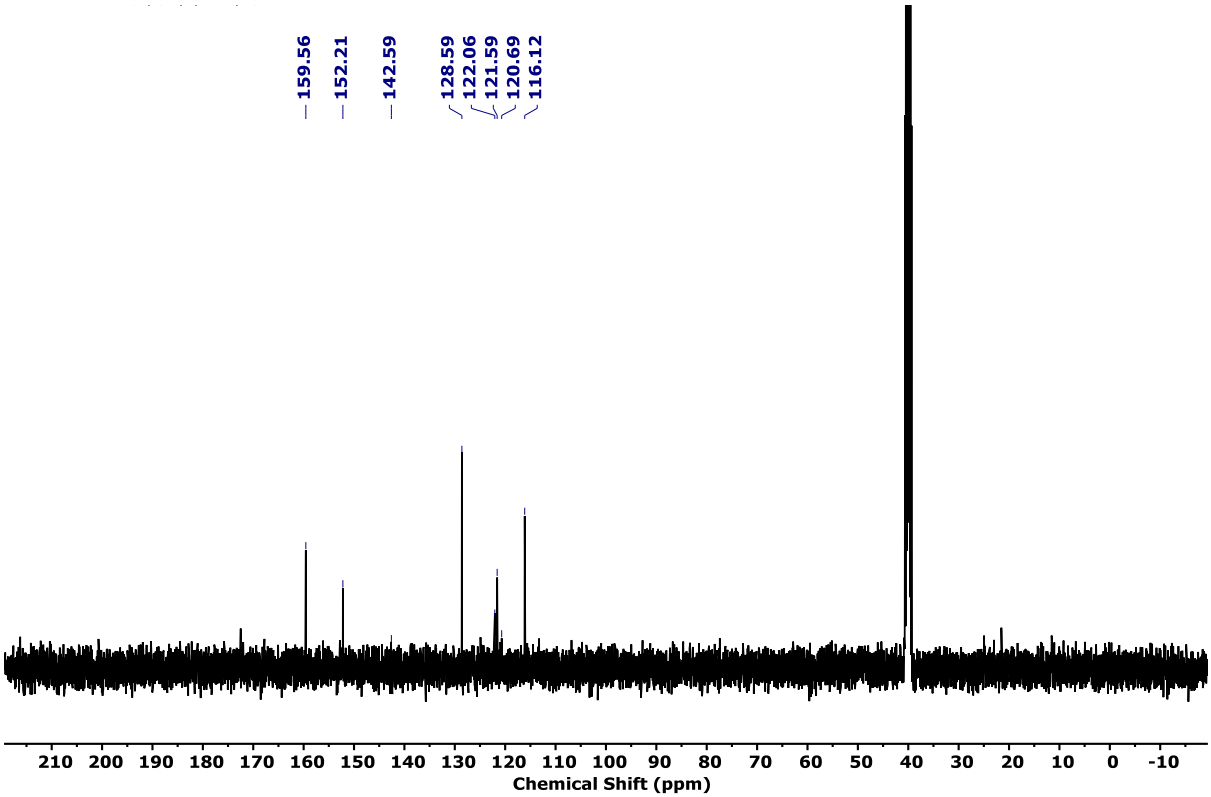

Figure 21. The ^{13}C NMR (100 MHz, DMSO-d_6) of 4-(1H-benzo[d]imidazol-2-yl)phenol (C).

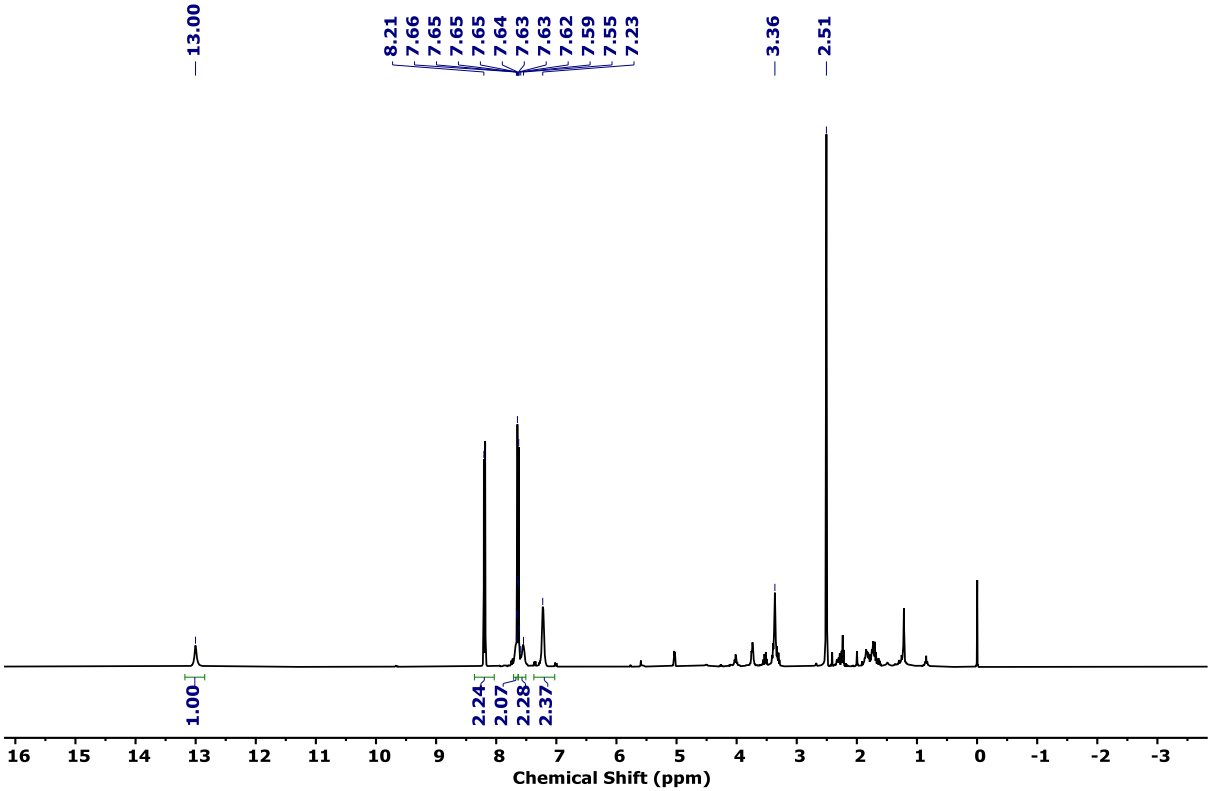

Figure 22. The ^{1}H NMR (400 MHz, DMSO-d_6) of 2-(4-chlorophenyl)-1H-benzo[d]imidazole (D).

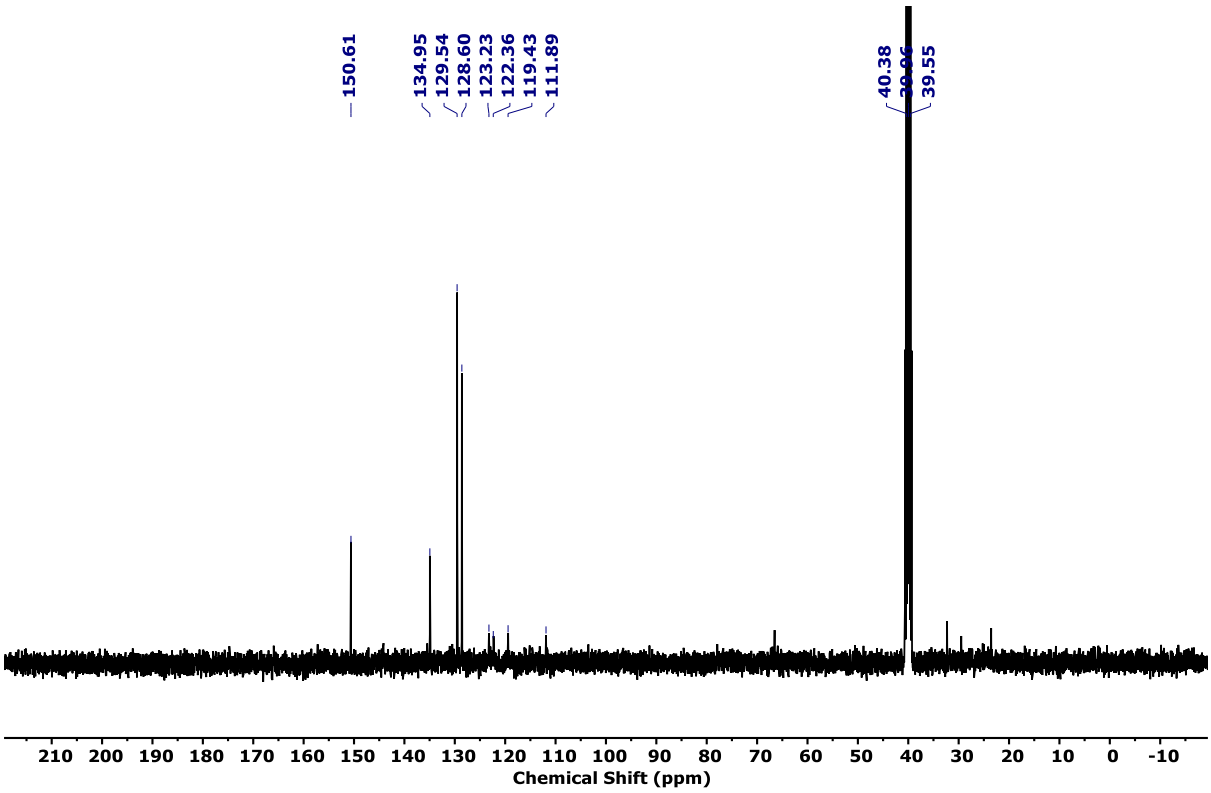

Figure 23. The ^{13}C NMR (100 MHz, DMSO-d_6) of 2-(4-chlorophenyl)-1H-benzo[d]imidazole (D).

3. Conclusion

We have successfully established that TAPT-BTD-COF can act as a decisive heterogeneous catalyst for the oxidative coupling between diamine and benzaldehyde. Synthesizing of this catalyst, low amount of catalyst loading, mild conditions, and significant yield of the respective products are the main features of this methodology. Further, this process provides us with straightforward and cheap access to a variety of Imidazole with moderate to good yields in mild conditions.

4. Acknowledgement

This work was done in collaboration with **Mr. Yogendra Nailwal** and is greatly acknowledged and respected.

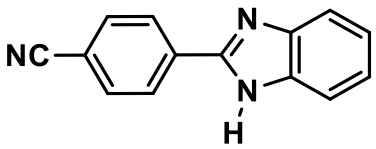

4-(1H-benzo[d]imidazol-2-yl)benzonitrile (A)

^{1}H NMR (400 MHz, DMSO-d_6): δ (ppm): 13.21 (s, 1H), 8.36 (d, J = 8.56 Hz, 2H), 8.05 (d, J = 8.6 Hz, 2H), 7.73 (d, J = 8.2 Hz, 1H), 7.58 (d, J = 7.64 Hz, 1H), 7.29 (d, J = 6.7 Hz, 2H). ^{13}C NMR (100 MHz, DMSO-d_6): δ (ppm): 149.83, 134.71, 133.49, 128.59, 127.45, 122.71, 119.83, 112.21.

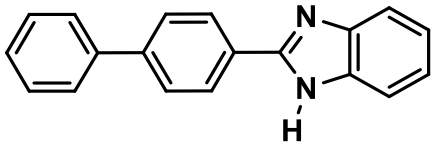

2-([1,1'-biphenyl]-4-yl)-1H-benzo[d]imidazole (B)

^{1}H NMR (400 MHz, DMSO-d_6): δ (ppm): 12.97 (s, 1H), 8.29 (d, J = 8.48 Hz, 2H), 7.89 (d, J = 8.44 Hz ,2H), 7.8 (d, J = 7.2 Hz 2H), 7.69 (d, J = 7.28 Hz, 1H), 7.51 (q, J = 7.99 Hz, 2H), 7.4 (t, J = 7.36 Hz, 1H), 7.22 (p, J = 5.63 Hz, 2H). ^{13}C NMR (100 MHz, DMSO-d_6): δ (ppm): 151.38, 141.76, 139.71, 133.79, 129.52, 128.39, 127.62, 122.18, 115.48.

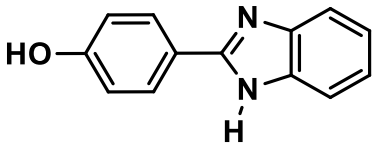

4-(1H-benzo[d]imidazol-2-yl)phenol (C)

^{1}H NMR (400 MHz, DMSO-d_6): δ (ppm): 12.63 (s, 1H), 9.94 (s, 1H), 8.00 (d, J = 8.64 Hz, 2H), 7.54 (dd, J = 4.6, 2.7 Hz, 2H), 7.16 (dd, J =3.12, 3.12 Hz, 2H), 6.91 (d, J = 8.68 Hz, 2H). ^{13}C NMR (100 MHz, DMSO-d_6): δ (ppm): 159.56, 152.21, 142.59, 128.59, 122.06, 121.59, 120.69, 116.12.

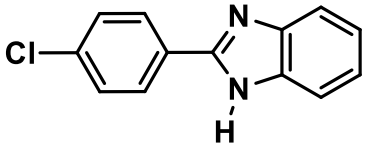

2-(4-chlorophenyl)-1H-benzo[d]imidazole (D)

^{1}H NMR (400 MHz, DMSO-d_6): δ (ppm): 13.00 (s, 1H), 8.21 (d, J = 8.0 Hz, 2H), 7.63 (d, J = 6.9 Hz, 4H), 7.23 (s, 2H). ^{13}C NMR (100 MHz, DMSO-d_6): δ (ppm): 150.61, 134.95, 129.54, 128.6, 123.36, 122.36, 119.43, 111.89.

Bibliography

1. Evans, A. M.; Strauss, M. J.; Corcos, A. R.; Hirani, Z.; Ji, W; Hamachi, L. S.; Aguilar-Enriquez, X.; Chavez, A. D.; Smith, B. J.; Dichtel, W.R. Two-Dimensional Polymers, and Polymerizations. *Chem. Rev.* **2022**, *122*, 1, 442–564.
2. Jhon, W.C.; Dichtel, W.R. Rationally Synthesized Two-dimensional Polymers. *Nature Chemistry* **2013**, *5*, 453–465.
3. Feng, X.; Ding X.; Jiang, D. Covalent Organic Frameworks. *Chem. Soc. Rev.*, **2012**, *41*, 6010–6022.
4. Ding, S. Y.; Wang, W.; Covalent organic frameworks (COFs): from design to applications. *Chem. Soc. Rev.*, **2013**, *42*, 548–568.
5. Segura, J. L.; Mancheno, M. J.; Zamora, F. Covalent organic frameworks based on Schiff-base chemistry: synthesis, properties, and potential applications. *Chem. Soc. Rev.*, **2016**, *45*, 5635-5671.
6. Diercks, C. S.; Yaghi, O. M. The atom, the molecule, and the covalent organic framework. *Science*, **2017**, *355*, eaal1585.
7. Lohse, M. S.; Bein, T. Covalent Organic Frameworks: Structures, Synthesis, and Applications. *Adv. Funct. Mater.* **2018**, *28*, 1705553.
8. Chaieb A., Halimi O., Bensouici A., Boudine B. B. B., Sahraoui B. Linear and nonlinear optical properties of the CdSe nanocrystals embedded in PMMA matrix. *Journal of Optoelectronics and Advanced Materials*, **2009**, *11*, 104-113.
9. Kandambeth, S.; Dey, K.; Banerjee, R. Covalent Organic Frameworks: Chemistry beyond the Structure. *J. Am. Chem. Soc.*, **2019**, *141*, 1807–1822.
10. Segura, J. L.; Royuela, S.; Ramos, M. M. Post-synthetic modification of covalent organic frameworks. Chem. Soc. Rev., 2019, 48,3903–3945.
11. Chen, W.; Wang, L.; Mo, D.; He, F.; Wen, Z.; Wu, X.; Xu, H.; L. Chen, L. Modulating Benzothiadiazole-Based Covalent Organic Frameworks via Halogenation for Enhanced Photocatalytic Water Splitting. *Angew. Chem. Int. Ed.* **2020**, *59*, 16902 – 16909.
12. Banerjee, T.;Gottschling, K.; Savasci, G.; Ochsenfeld, C.; Lotsch B. V. H_2 Evolution with Covalent Organic Framework Photocatalysts. *ACS Energy Lett.* **2018**, *3*, 400−409.
13. Unterlass M. M. Hot Water Generates Crystalline Organic Materials. *Angew. Chem. Int. Ed.* **2018**, *57*, 2292–2294.
14. Abuzeid, H. R.; El-Mahdy, A. F. M.; Kuo, S. W.; Covalent organic frameworks: Design principles, synthetic strategies, and diverse applications. *Giant 6*, **2021**, 100054.
15. Wang, G. B.; Li, S.; Yan, C. X.; Zhu, F.C.; Lin, Q. Q.; Xie, K. H.; Geng, Y.; Dong Y. B. Covalent organic frameworks: emerging high-performance platforms for efficient photocatalytic applications. *J. Mater. Chem. A*, **2020**, *8*, 6957.
16. Guo, J.; Jiang, D. Covalent Organic Frameworks for Heterogeneous Catalysis: Principle, Current Status, and Challenges. *ACS Cent. Sci.* **2020**, *6*, 869−879.
17. Wang, P.-L.; Ding, S.-Y.; Zhang, Z.-C.; Wang, Z.-P.; Wang W. Constructing Robust Covalent Organic Frameworks via Multicomponent Reactions. *J. Am. Chem. Soc.* **2019**, *141*, 18004−18008.

18. Mohamed, G. M.; EL-Mahdy, A. F. M.; Kotp, M. G.; Kuo, S.-W. Advances in porous organic polymers: syntheses, structures, and diverse applications. *Mater. Adv.*, **2022**, *3*, 707
19. Das; S.; Heasman, P.; Ben, T.; Qiu S. Porous Organic Materials: Strategic Design and Structure−Function Correlation. *Chem. Rev.* **2017**, *117*, 1515−1563.
20. Rodríguez-San-Miguel, D.; Zamora, F. Processing of Covalent Organic Frameworks: An Ingredient for a Material to Succeed. *Chem. Soc. Rev.* **2019**, *48*, 4375−4386
21. Geng, K.; He, T.; Liu, R.; Dalapati, S.; Tan, K. T.; Li, Z.; Tao, S.; Gong, Y.; Jiang, Q.; Jiang D. Covalent Organic Frameworks: Design, Synthesis, and Functions, *Chem. Rev.* **2020**, *120*, 8814−8933
22. Côte, A. P.; El-Kaderi, H. M.; Furukawa, H.; Hunt, J. R.; Yaghi, O.́ M. Reticular Synthesis of Microporous and Mesoporous 2D Covalent Organic Frameworks. J. Am. Chem. Soc. 2007, 129, 12914−12915
23. Pang, Z. F.; Xu, S. Q.; Zhou, T. Y.; Liang, R. R.; Zhan, T. G.; Zhao, X. Construction of Covalent Organic Frameworks Bearing Three Different Kinds of Pores through the Heterostructural Mixed Linker Strategy. *J. Am. Chem. Soc.* **2016**, *138*, 4710−3
24. Zhang, K. D.; Matile, S. Complex Functional Systems with Three Different Types of Dynamic Covalent Bonds. *Angew. Chem., Int. Ed.* **2015**, *54*, 8980−3
25. Xu, L. Q.; Ding, S. Y.; Liu, J. M.; Sun, J. L.; Wang, W.; Zheng, Q. Y. Highly Crystalline Covalent Organic Frameworks from Flexible Building Blocks. *Chem. Commun.* **2016**, *52*, 4706−4709
26. Ren, S.; Bojdys, M. J.; Dawson, R.; Laybourn, A.; Khimyak, Y. Z.; Adams, D. J.; Cooper, A. I. Porous, Fluorescent, Covalent Triazine Based Frameworks via Room-Temperature and Microwave-Assisted Synthesis. *Adv. Mater.* **2012**, *24*, 2357−61
27. Chandra, S.; Kandambeth, S.; Biswal, B. P.; Lukose, B.; Kunjir, S. M.; Chaudhary, M.; Babarao, R.; Heine, T.; Banerjee, R. Chemically Stable Multilayered Covalent Organic Nanosheets from Covalent Organic Frameworks via Mechanical Delamination. *J. Am. Chem. Soc.* **2013**, *135*, 17853−17861
28. Guan, X.; Ma, Y.; Li, H.; Yusran, Y.; Xue, M.; Fang, Q.; Yan, Y.; Valtchev, V.; Qiu, S. Fast, Ambient Temperature and Pressure Ionothermal Synthesis of Three-Dimensional Covalent Organic Frameworks. *J. Am. Chem. Soc.* **2018**, *140*, 4494−4498
29. Bi, S., Yang, C., Zhang, W. *et al.* Two-dimensional semiconducting covalent organic frameworks via condensation at aryl methyl carbon atoms. *Nat Commun 10***,** 2467 (**2019**)
30. Feng, X.; Chen, L.; Honsho, Y.; Saengsawang, O.; Liu, L.; Wang, L.; Saeki, A.; Irle, S.; Seki, S.; Dong, Y.; Jiang, D. An Ambipolar Conducting Covalent Organic Framework with Self-Sorted and Periodic Electron Donor-Acceptor Ordering, *Adv. Mater.* **2012**, *24*, 3026–3031
31. Guo, J.; Xu, Y.; Jin, S.; Chen, L.; Kaji, T.; Honsho, Y.; Addicoat, M. A.; Kim, J.; Saeki, A.; Ihee, H.; Seki, S.; Irle, S.; Hiramoto, M.; Gao, J.; Jiang, D. Conjugated Organic Framework with Three-Dimensionally Ordered Stable Structure and Delocalized π Clouds. *Nat. Commun.* **2013**, *4*, 2736
32. Dalapati, S.; Jin, E.; Addicoat, M.; Heine, T.; Jiang, D. Highly Emissive Covalent Organic Frameworks. *J. Am. Chem. Soc.* **2016**, *138*, 5797−5800
33. Kaleeswaran, D.; Vishnoi, P.; Murugavel, R. [3 + 3] Imine and β-Ketoenamine Tethered Fluorescent Covalent-Organic Frameworks for CO_2 Uptake and Nitroaromatic Sensing. *J. Mater. Chem. C* **2015**, *3*, 7159−7171
34. Zhang, Y.; Riduan, S. N.; Wang, J. Redox-Active Metal− and Covalent Organic Frameworks for Energy Storage: Balancing Porosity and Electrical Conductivity. *Chem. - Eur. J.* **2017**, *23*, 16419−16431

35. Lee, J.-Y.; Wood, C. D.; Bradshaw, D.; Rosseinsky, M. J.; Cooper, A. I. Hydrogen Adsorption in Microporous Hypercrosslinked Polymers. *Chem. Commun.* **2006**, 2670−2672
36. Rogge, S. M. J.; Bavykina, A.; Hajek, J.; Garcia, H.; OlivosSuarez, A. I.; Sepulveda-Escribano, A.; Vimont, A.; Clet, G.; Bazin, P.;́ Kapteijn, F.; et al. Metal−Organic and Covalent Organic Frameworks as Single−Site Catalysts. *Chem. Soc. Rev.* **2017**, *46* (11), 3134−3184
37. Liras, M.; Barawi, M.; de la Peña O'Shea, V. A. Hybrid Materials Based on Conjugated Polymers and Inorganic Semiconductors as Photocatalysts: from Environmental to Energy Applications. *Chem. Soc. Rev.* **2019**, *48*, 5454−5487
38. Battula, V. R.; Singh, H.; Kumar, S.; Bala, I.; Pal, S. K.; Kailasam K. Natural Sunlight Driven Oxidative Homocoupling of Amines by a Truxene-Based Conjugated Microporous Polymer. *ACS Catal.* **2018**, *8*, 6751−6759
39. Han, S.; Li, Z.; Ma, S.; Zhi, Y.; Xia, H.; Chen, X.; Liu, X. Bandgap engineering in benzotrithiophene-based conjugated microporous polymers: a strategy for screening metal-free heterogeneous photocatalysts. *J. Mater. Chem. A*, **2021**, *9*, 3333
40. Chen, W.; Yang, Z.; Xie, Z.; Li, Y.; Yu, X.; Lua, F.; Chen, L. Benzothiadiazole functionalized D–A type covalent organic frameworks for effective photocatalytic reduction of aqueous chromium(VI). *J. Mater. Chem. A*, **2019**, *7*, 998
41. Wang, L.; Xia, Q.; Hou, M.; Yan, C.; Xu, Y.; Qu, J.; Liu, R. A photostable cationic fluorophore for long-term bioimaging. *J. Mater. Chem. B*, **2017**, *5*, 9183